C H A P T E R - VII

ANALYSIS, DISCUSSIONS AND CONCLUSIONS

7.1.0. GENERAL

One of the principal aim of the present research project is to inquire into whether there is a specific criterion of failure for jointed rocks, whether there is a possibility to express it into a mathematically amenable form and whether it approximates to any of the well recognized failure criteria for materials so as to take the advantage of the established mathematical frame work for the solution of varieties of boundary value problems. For fundamental understanding it is essential to delineate the mechanism of shearing in jointed rocks and to investigate the influence of principal factors and its implications on the stability of jointed rocks. The rational approach shall be to analyse the experimental investigations on the laboratory specimens against the theoretical model developed to produce answers to various questions stated above and to determine the extent to which the theoretical conceptulization agree and how far the conclusions can be extended to make possible for their utilization towards the solution of engineering problems concerned with jointed rocks. The values from analysis are presented in consolidated form through tables 7.1 to 7.3.

TABLE - 7.1

Gouge material	α°	Cell pressure σ_3 kg/cm^2	Major stress σ_1 kg/cm^2	$\sigma_1-\sigma_3$ kg/cm^2	$\sigma_1+\sigma_3$ kg/cm^2	χ kg/cm^2	ψ°
1	2	3	4	5	6	7	8
C:S 1:2	54.8°	2	55.68	53.68	57.68	22	28°
		4	59.53	55.53	63.53		
		6	69.86	63.86	75.86		
C:S 1:2	45°	2	73.57	71.57	75.57	25	31°
		4	77.30	73.30	81.30		
		6	82.08	76.08	88.08		
C:S 1:2	30°	2	86.84	84.84	88.84	93	26°
		4	192.81	188.81	196.81		
		6	283.66	277.66	289.66		
C:S 1:3	54.8°	2	32.23	30.23	34.23	11	28°
		4	34.85	30.85	38.85		
		6	58.76	52.76	64.76		
C:S 1:3	45°	2	31.62	29.62	33.62	15	31°
		4	37.94	33.94	41.94		
		6	62.64	56.64	68.64		
C:S 1:3	30°	2	45.50	43.50	47.50	43	26°
		4	94.70	90.70	98.70		
		6	118.17	112.17	124.17		
C:S 1:4	54.8°	2	16.81	14.81	18.81	4.5	28°
		4	21.90	17.90	25.90		
		6	35.43	29.43	41.43		
C:S 1:4	45°	2	22.67	20.67	24.67	6.0	31°
		4	30.22	26.22	34.22		
		6	36.54	30.54	42.54		
C:S 1:4	30°	2	82.21	80.21	84.21	39	26°
		4	87.60	83.60	91.60		
		6	35.43	29.43	41.43		

C kg/cm^2	ϕ°	Dilatancy $\mathfrak{D}$	$\frac{\sigma_1}{\mathfrak{D}}$ kg/cm^2	$\frac{\sigma_1}{\mathfrak{D}} - \sigma_3$ kg/cm^2	$\frac{\sigma_1}{\mathfrak{D}} + \sigma_3$ kg/cm^2	χ^*	$\psi^{\circ *}$
9	10	11	12	13	14	15	16
			65.35	63.35	67.35		
12.98	32.1°	0.852	69.87	65.87	73.87	32	25°
			82.00	76.00	88.00		
			122.41	120.41	124.41		
15.65	37°	0.601	128.62	124.62	132.62	63	25°
			136.57	130.57	142.57		
			90.46	88.46	92.46		
53.24	29.2°	0.961	200.84	196.84	204.84	100	25°
			295.48	289.48	301.48		
			37.82	35.82	39.82		
6.49	32.1°	0.852	40.90	36.90	44.90	17	25°
			68.97	62.97	74.97		
			52.61	50.61	54.61		
9.39	37°	0.601	63.13	59.13	67.13	28	25°
			104.23	98.23	110.23		
			47.40	45.40	49.40		
24.62	29.2°	0.961	98.58	94.58	102.58	46	25°
			123.09	117.09	129.09		
			19.73	17.73	21.73		
2.66	32.1°	0.852	25.70	21.70	29.70	8	25°
			41.58	35.58	47.58		
			37.72	35.72	39.72		
3.76	37°	0.601	50.28	46.28	54.28	21	25°
			60.80	54.80	66.80		
			85.63	83.63	87.63		
22.33	29.2°	0.961	91.15	87.15	95.15	42	25°
			36.91	30.91	42.91		

$\overset{*}{C}$	ϕ_μ°	$J_1 = \frac{\sigma_1}{D} + 2\sigma_3$	$J_2 = \sqrt{\frac{2\sigma_1}{D}\sigma_3 + \sigma_3^2}$	λ°	K	C_j kg/cm^2	ϕ_j° kg/cm^2
17	18	19	20	21	22	23	24
		69.35	16.29				
18.13	28°	77.87	23.98	9°	14	15.98	28.48°
		94.00	31.94				
		126.41	22.22				
35.69	28°	136.62	32.32	9°	16	18.26	28.48°
		148.57	40.92				
		94.46	19.13				
56.65	28°	208.84	40.28	9°	18	20.54	28.48°
		307.48	59.80				
		41.82	12.46				
9.63	28°	48.90	18.52	9°	8	9.13	28.48°
		80.97	29.39				
		56.61	14.64				
15.86	28°	71.13	22.83	9°	12	13.78	28.48°
		116.23	35.87				
		51.40	13.91				
26.00	28°	106.58	28.37	9°	16	18.26	28.48°
		135.09	38.90				
		23.73	9.11				
4.53	28°	33.70	14.88	9°	5	5.70	28.48°
		53.58	23.13				
		41.72	12.44				
11.90	28°	58.28	20.45	9°	8	9.13	28.48°
		72.80	27.67				
		89.63	18.62				
23.79	28°	99.25	27.30	9°	12	13.70	28.48°
		78.91	19.31				

TABLE - 7.2

Gouge material	α°	Cell pressure $\bar{\sigma_3}$ kg/cm^2	Major stress $\bar{\sigma_1}$ kg/cm^2	$\bar{\sigma_1}-\bar{\sigma_3}$ kg/cm^2	$\bar{\sigma_1}+\bar{\sigma_3}$ kg/cm^2	χ kg/cm^2	ψ°
1	2	3	4	5	6	7	8
N_x 50:50	54.8°	2	19.03	17.03	21.03	9.5	23°
		4	25.84	21.84	29.84		
		6	31.07	25.07	37.07		
		8	51.01	43.01	59.01		
40:60	54.8°	2	6.60	4.60	8.60	2.0	21°
		4	19.18	15.18	23.18		
		6	17.27	11.27	23.27		
		8	46.46	38.46	54.46		
30:70	54.8°	2	5.70	3.70	7.70	7.50	18°
		4	7.80	3.80	11.80		
		6	23.33	17.33	29.33		
		8	26.86	18.86	34.86		
A_x 50:50	54.8°	2	11.85	9.85	13.85	4.5	23°
		4	17.43	13.43	21.43		
		6	24.23	18.23	30.23		
		8	26.05	18.05	34.05		
40:60	54.8°	2	6.85	4.85	8.85	3.0	21°
		4	14.67	10.67	18.67		
		6	18.31	12.31	24.31		
		8	22.71	14.71	30.71		
30:70	54.8°	2	10.47	8.47	12.47	4.0	18°
		4	9.74	5.74	13.74		
		6	17.94	11.94	23.94		
		8	51.50	43.50	59.50		

C	ø	Dila-tancy	$\frac{\sigma_1}{D}$	$\frac{\sigma_1}{D} - \sigma_3$	$\frac{\sigma_1}{D} + \sigma_3$	χ^*	ψ^*
kg/cm^2	degree	D	kg/cm^2	kg/cm^2	kg/cm^2	kg/cm^2	degree
9	10	11	12	13	14	15	16
5.15	25.1°	0.967	19.67 26.72 32.15 52.75	17.67 22.72 26.15 44.75	21.67 30.72 38.15 60.75	11.5	20°
1.071	22.5	0.967	6.83 19.83 17.86 48.05	4.83 15.83 11.86 40.05	8.83 23.83 23.86 56.05	3.50	20°
3.94	19°	0.967	5.90 8.07 24.13 27.78	3.90 4.07 18.13 19.78	7.90 12.07 30.13 35.78	7.0	20°
2.44	25.1°	0.967	12.25 18.02 25.06 26.94	10.25 14.02 19.06 18.94	14.25 22.02 31.06 34.94	6.5	20°
1.61	22.5°	0.967	7.08 15.17 18.93 23.49	5.08 11.17 12.93 15.49	9.08 19.17 24.93 31.49	4.0	20°
2.10	19°	0.967	10.83 10.07 18.55 53.26	8.83 6.07 12.55 45.26	12.83 14.07 24.55 61.26	3.5	20°

$\overset{*}{C}$	ϕ_μ	$J_1 = \frac{\sigma_1}{p} + 2\sigma_3$	$J_2 = \sqrt{\frac{2\sigma_1}{p}\sigma_3 + \sigma_3^2}$	λ°	K	C_j	ϕ_j°
kg/cm^2					kg/cm^2	kg/cm^2	
17	18	19	20	21	22	23	24
6.12	21.4°	23.67 34.72 44.15 68.72	9.09 15.15 20.53 30.13	9°	10	8.196	21.20
1.87	21.4°	10.83 27.83 29.86 64.05	5.60 13.22 15.82 28.86	9°	7	5.73	21.20
3.72	21.4°	9.90 16.07 35.09 43.78	5.25 8.98 17.69 22.55	9°	5	4.09	21.20
3.46	21.4°	16.25 26.02 37.06 42.94	7.28 12.66 18.35 23.30	9°	10	8.196	21.20
2.13	21.4°	11.08 23.17 30.93 39.49	5.69 11.72 16.22 20.97	9°	7	5.73	21.20
1.860	21.4°	14.83 18.07 30.55 69.26	6.88 9.83 16.08 30.27	9°	5	4.09	21.20

TABLE - 7.3

Gouge material	Designation	Cell pressure σ_3 kg/cm^2	Major stress σ_1 kg/cm^2	$\sigma_1-\sigma_3$ kg/cm^2	$\sigma_1+\sigma_3$ kg/cm^2	χ kg/cm^2	$\varphi°$
1	2	3	4	5	6	7	8
1:3	$B_4^{54.8}$*	4	32.15	28.15	36.15	-	-
	$B_4^{54.8}$**	4	27.32	23.32	31.32	-	-
	$B_4^{54.8}$***	4	79.18	75.18	83.18	-	-
1:3	B_2^{45}*	2	10.94	8.94	12.94		
	B_4^{45}**	4	18.02	14.02	22.02	1	31°
	B_6^{45}***	6	40.38	34.38	46.38		
1:3	B_4^{30}*	4	175.61	171.61	179.61	-	-

* Monotonic load application till failure.

** Triangular load application, after every two cycles the load is increased and repeated till failure.

*** Sinusoidal load application, after every two cycles the load is increased and repeated till failure.

Note: The above tests are performed by employing closed loop servo controlled MTS setup.

C	ø	Dilatancy D	$\frac{\sigma_1}{p}$	$\frac{\sigma_1}{p} - \sigma_3$	$\frac{\sigma_1}{p} + \sigma_3$	χ^*	ψ^*
kg/cm^2	degree		kg/cm^2	kg/cm^2	kg/cm^2	kg/cm^2	degree
9	10	11	12	13	14	15	16
-	-	0.848	36.95	32.95	40.95	-	-
-	-	0.896	31.40	27.40	35.40	-	-
-	-	0.865	91.01	87.01	95.01	-	-
		Av.0.870					
		0.606	17.84	15.84	19.84		
0.626	37°	0.630	29.38	25.38	33.38	24.50	9°
		0.604	65.84	59.84	71.84		
		Av.0.6133					
-	-	0.967	181.60	177.60	185.60	-	-

C^*	ϕ_μ	$J_1 = \frac{\sigma_1}{D} + 2\sigma_3$	$J_2 = \sqrt{\frac{2\sigma_1}{D}\sigma_3 + \sigma_3^2}$	λ°	K	C_j	ϕ_j°
						kg/cm^2	kg/cm^2
17	18	19	20	21	22	23	24
-	-	44.95	17.65	-	-	-	-
-	-	39.40	16.35	-	-	-	-
-	-	99.01	28.43	-	-	-	-
		22.2	8.76				
5.04	27°	37.98	12.96	8.5	6	6.67	26.50
		79.19	28.74				
-	-	189.60	38.32	-	-	-	-

7.2.0. A FAILURE CRITERION FOR JOINTED ROCKS

During the present investigations a failure criterion has been developed from the equilibrium conditions of a body sliding on an inclined plane. To incorporate the fundamental phenomenon of dilatancy in jointed rocks it is postulated that the energy associated with dilatancy is the excess energy expended in sliding at an orientation deviating from the critical orientation associated only with the surface friction between two sliding bodies. Figures 7.1 to 7.5 depict the plots produced on the basis of conventional and derived failure expression on Coulomb space. It is clearly evident that the derived expression succeed in separating the basic angle of friction between the two surfaces as an intrinsic property. The exposition stands proved resonably against the experimental investigations conducted on jointed rock specimens at three different joint orientations with the horizontal viz. 54.8°, 45° and 30° for two varieties of materials, with three to four (2,4,6 kg/cm^2) (2, 4, 6, 8 kg/cm^2) different cell pressures and also for specimens having N_x and A_x sizes. Thus the main plank of the mechanistic model remains still based on the Coulomb's classical conception for friction between bodies. It bears out from the experimental investigations that the energy beyond the energy spent in friction is a geometrical parameter. At the instant of failure the critical combinations of stresses are modified in proportion to this geometrical parameter. If the energy spent in the basic friction is a slope quantity of the failure envelope then the excess energy due to dilatancy is getting amalgamated into the

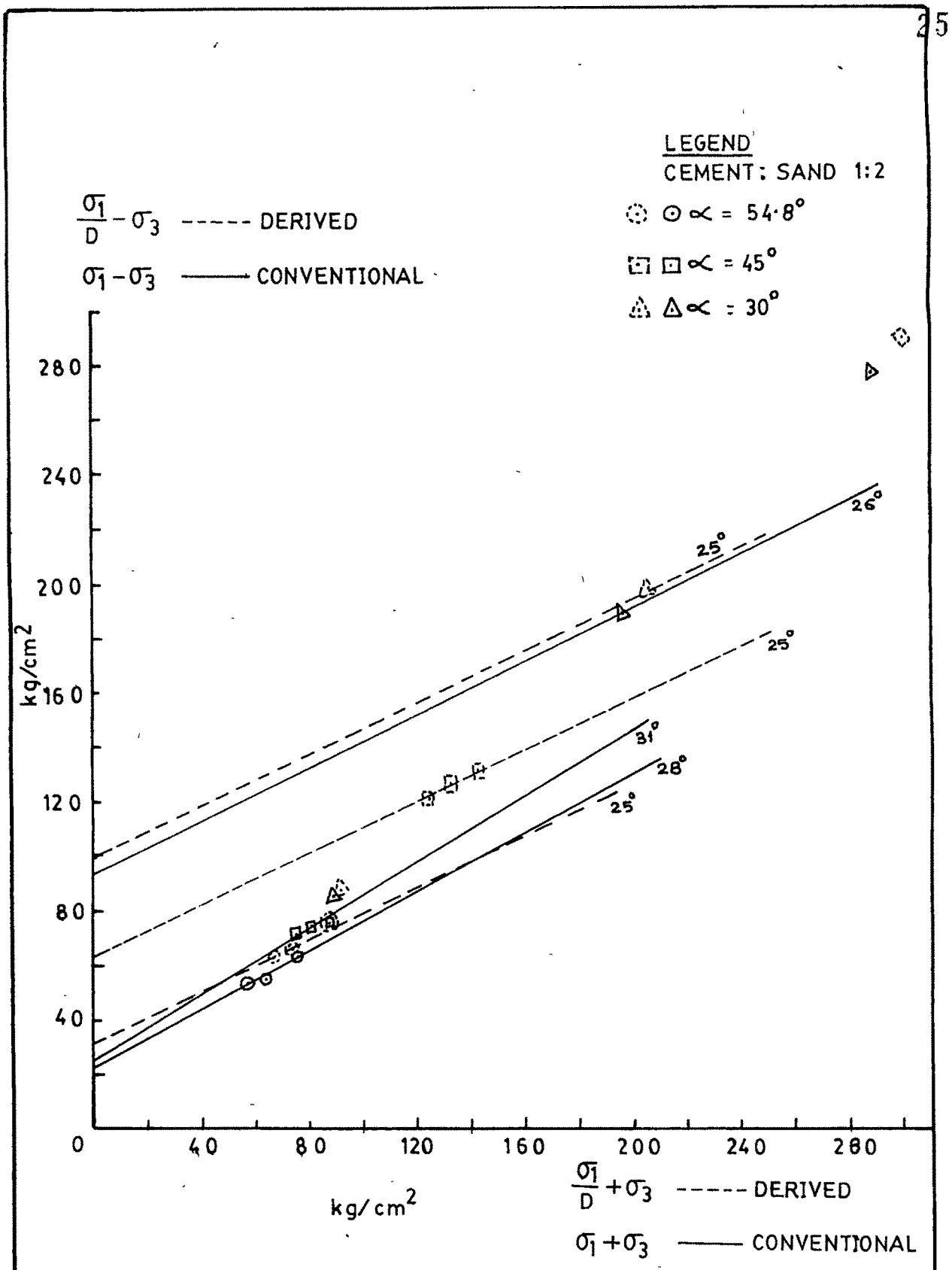

FIG.7·1 A COMPARISION OF FAILURE ENVELOPES

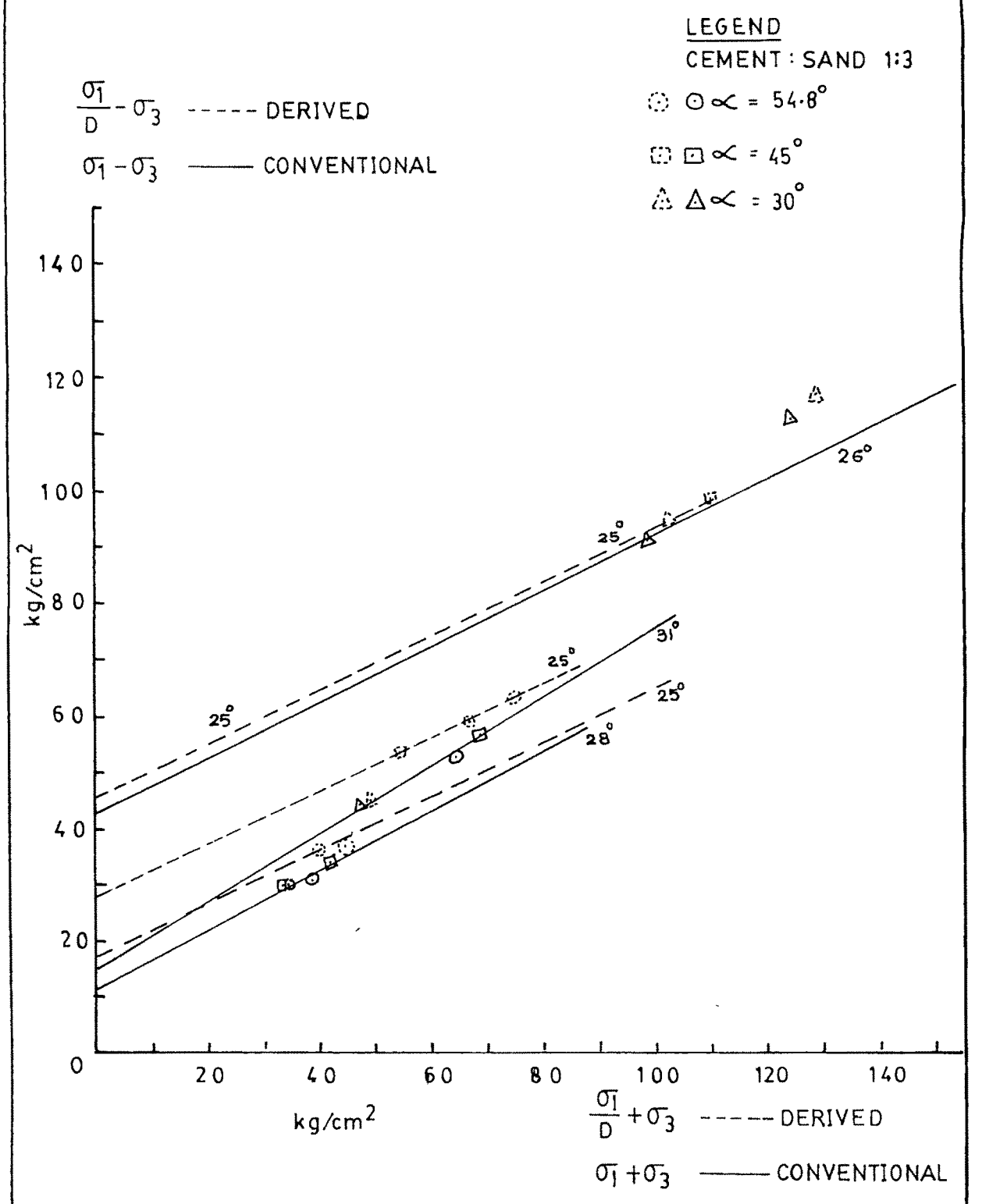

FIG.7·2 A COMPARISION OF FAILURE ENVELOPES

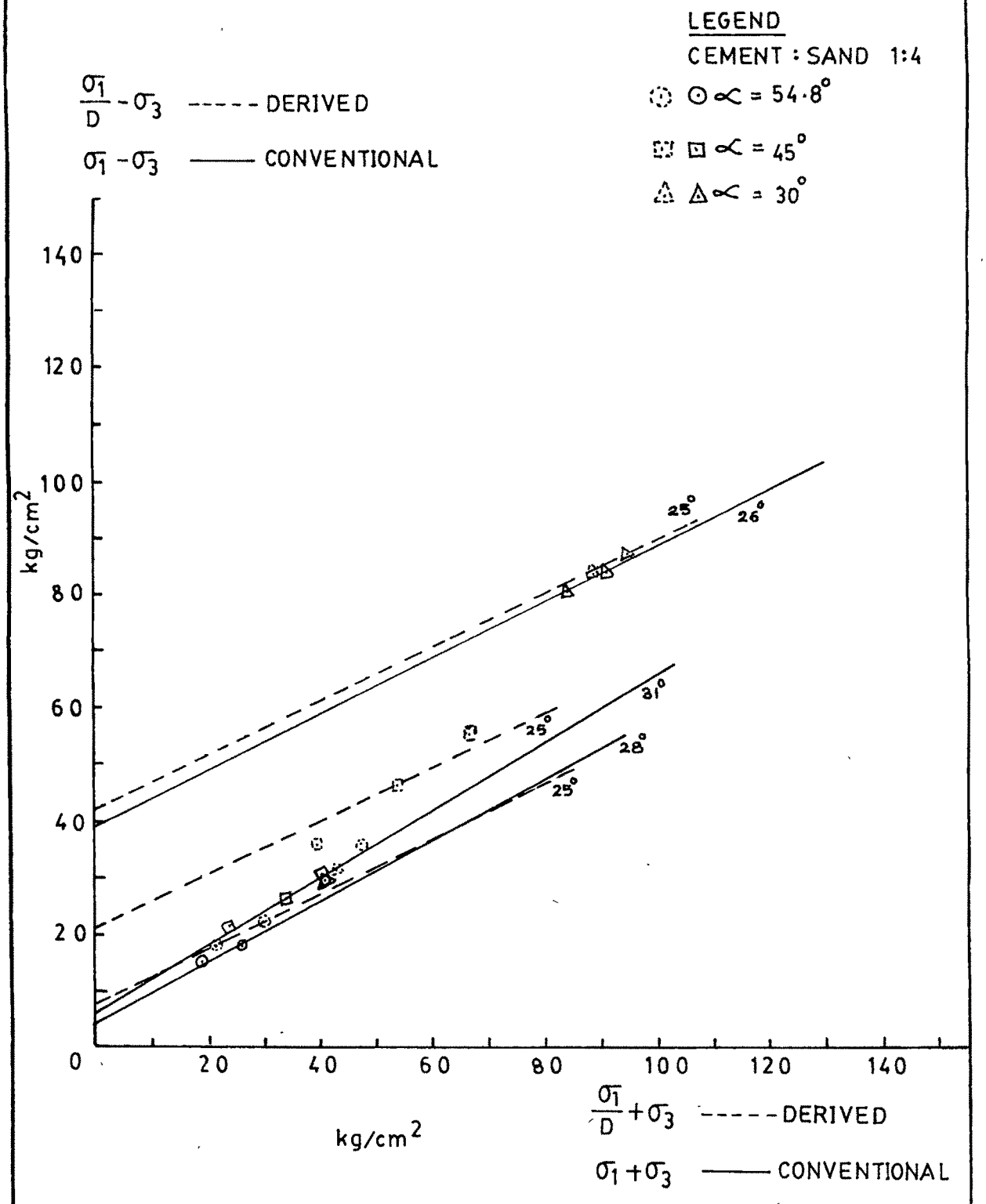

FIG.7·3 A COMPARISION OF FAILURE ENVELOPES

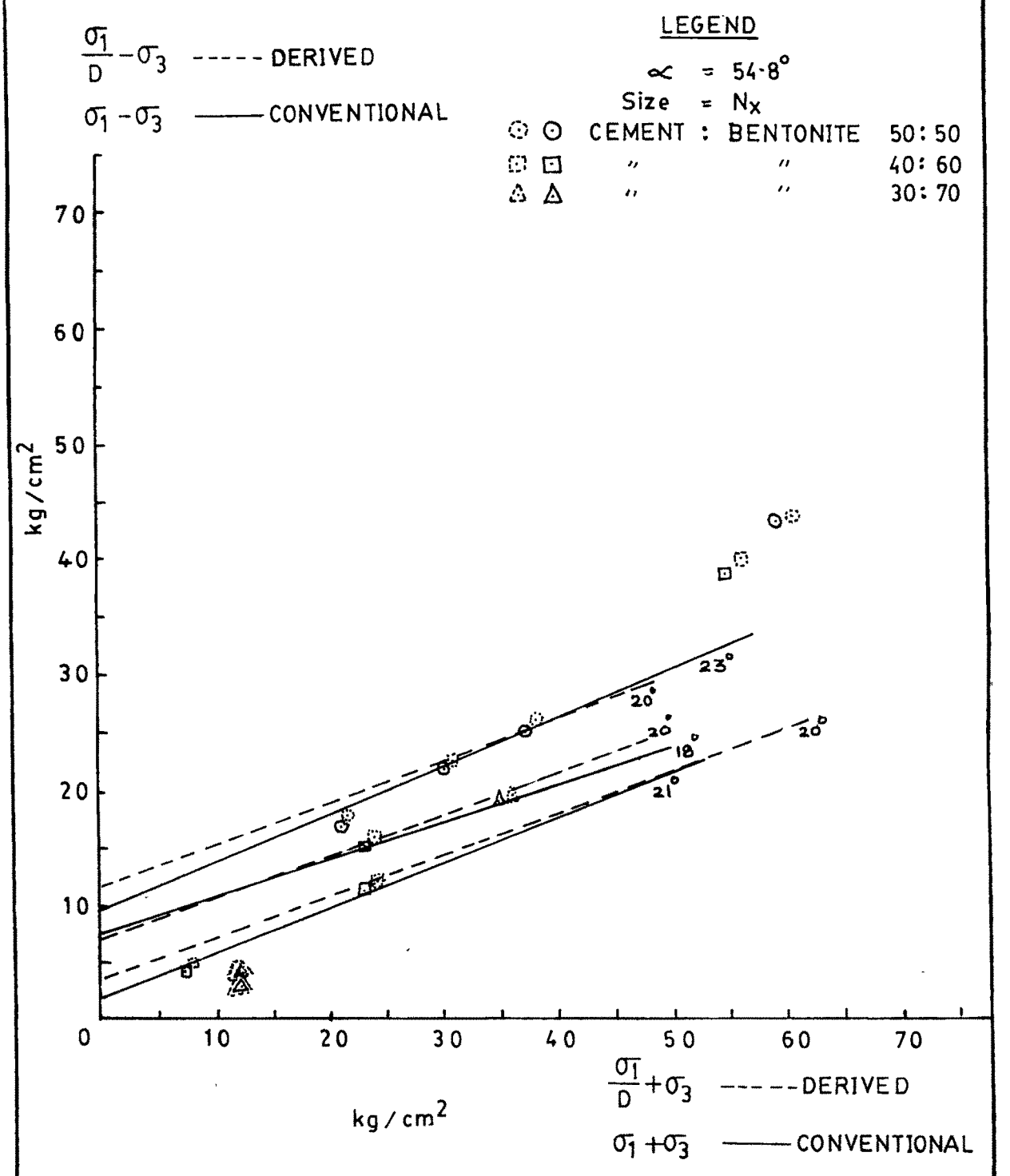

FIG.7·4 A COMPARISION OF FAILURE ENVELOPES

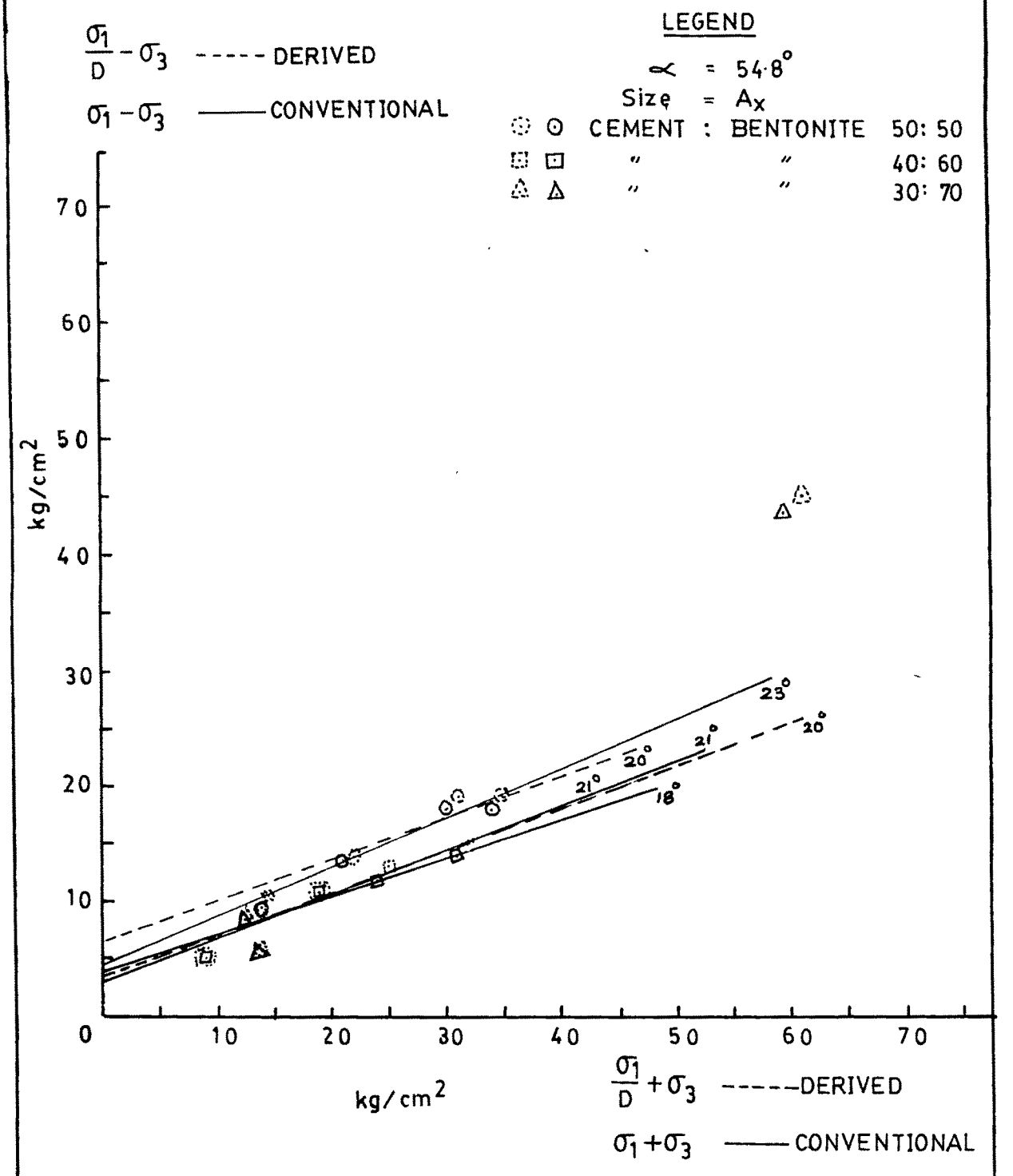

FIG.7·5 A COMPARISION OF FAILURE ENVELOPES

intercept quantity. Thus the Coulomb equation for failure envelope should be expressed as:

$$\tau_f = \overset{*}{C} + \sigma_f \tan \phi_\mu \qquad \ldots.7.2.1$$

Where $\overset{*}{C}$ is an intercept inclusive of energy in excess of basic frictional energy. This permits to retain the mathematical structure of plasticity intact only it gets truncated owing to the influence of all the factors other than the basic friction angle. Hence the step ahead is to explore the possibility of a mathematically convenient expression in terms of stress invariants for exploitation towards the solution of stability problems even by limit equilibrium methods. In Drucker-Prager approximation of the Mohr-Coulomb criterion such a possibility exists. Figures 7.6 to 7.10 are the plots prepared from the approximations inscribring the Mohr-Coulomb and circumscribing the Mohr-Coulomb failure space. Experimental results when plotted on these basis indicate that the softer gouge material (cement-bentonite) tend to follow the Drucker-Prager approximation circumscribing Mohr-Coulomb criterion, while the harder material (cement-sand) tends to follow the Drucker-Prager approximation inscribing Mohr-Coulomb failure criterion. Since it has been possible to express the failure criterion in terms of stress-invariants a fundamental step has been accomplished of removal of restrictions getting imposed owing to the testing conditions. The implication of validity of Drucker-Prager approximation to the classical Mohr-Coulomb criterion is thus the availability of the entire mathematical framework developed under the umbrella of theory of plasticity for the solution of boundary value problems concerning jointed rock. Nevertheless in order to exploit

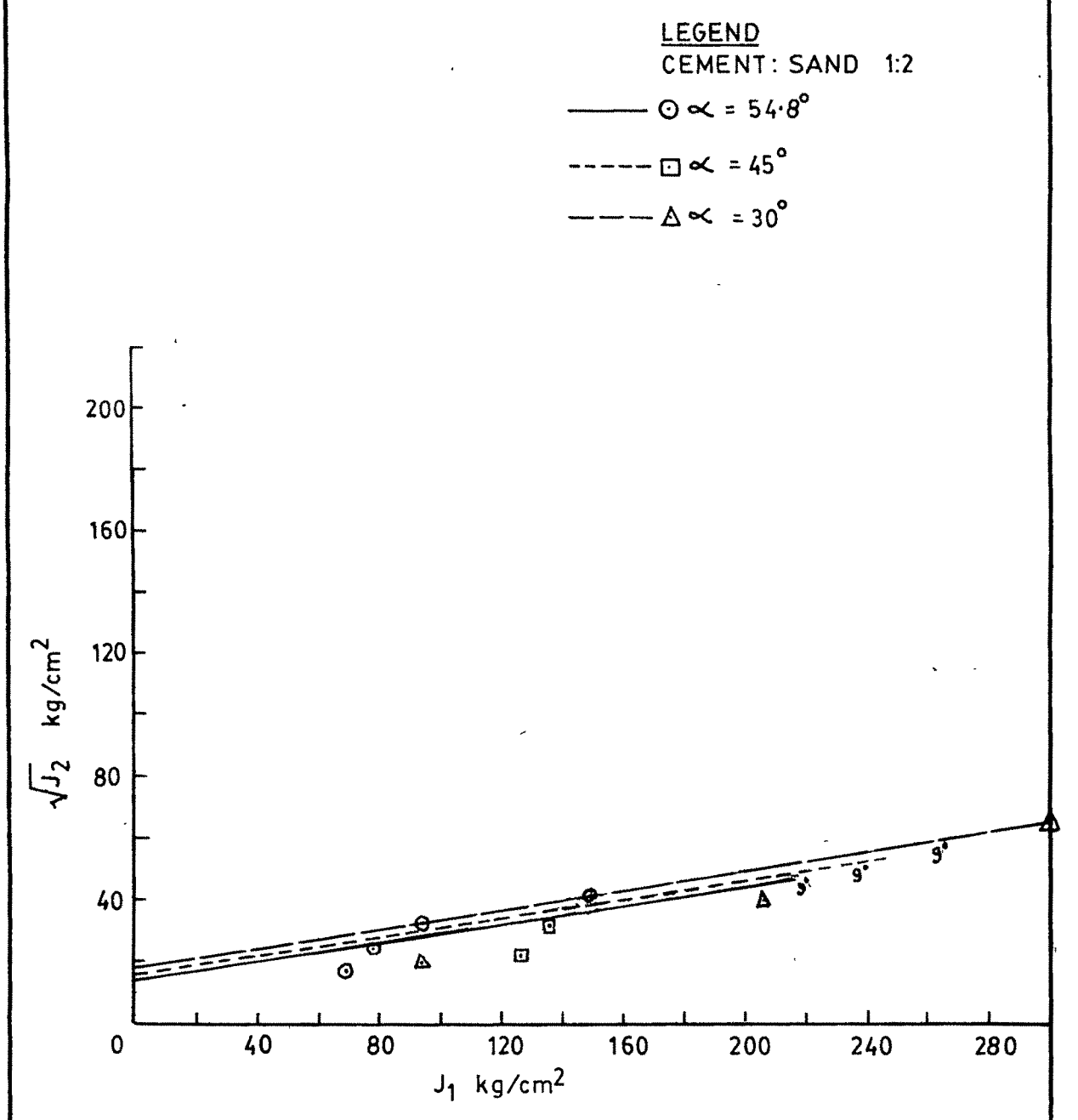

FIG·7·6 A FAILURE ENEVELOPE IN TERMS OF STRESS INVARIENTS (Drucker-Prager approximation)

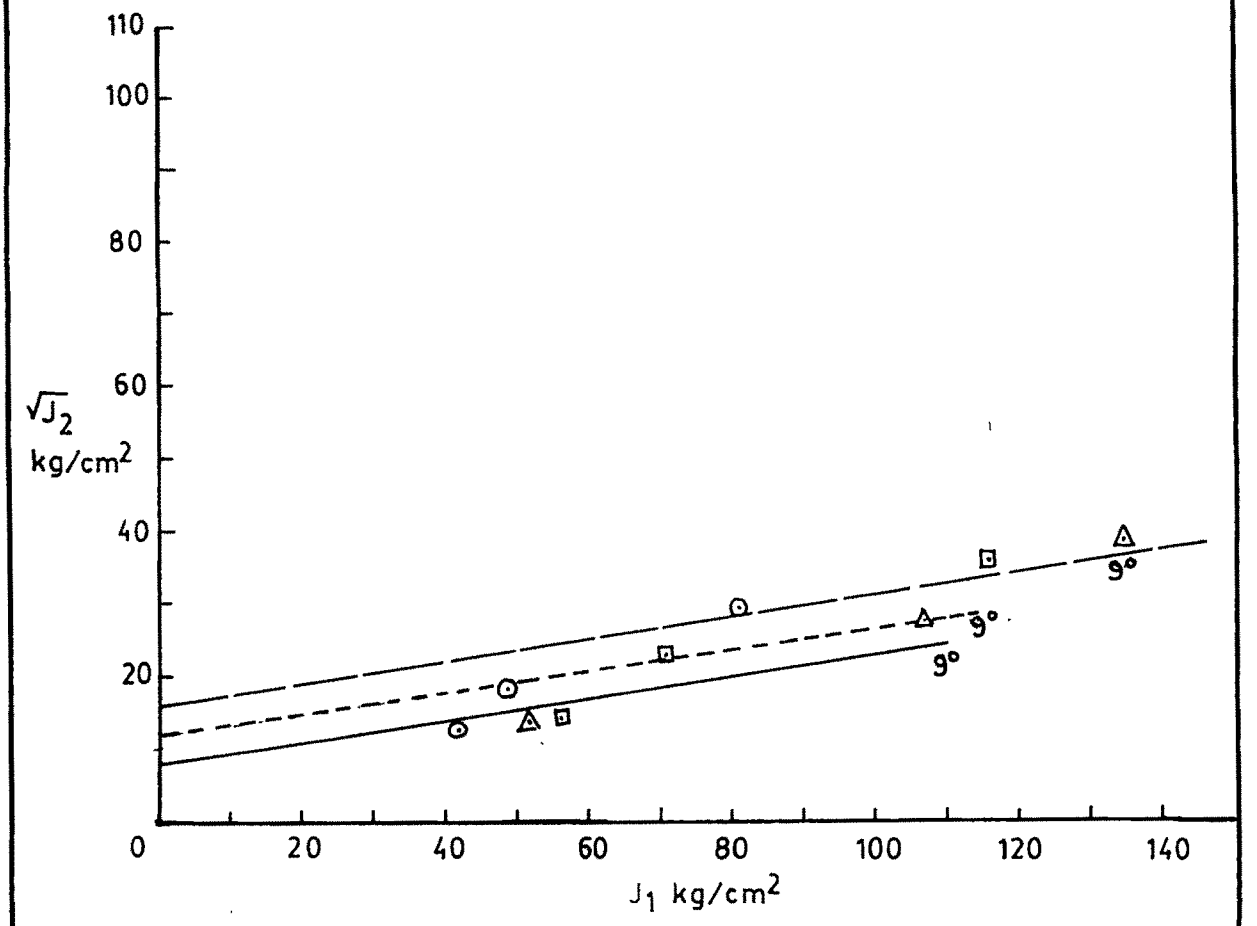

FIG-7·7 A FAILURE ENEVELOPE IN TERMS OF STRESS INVARIENTS
(Drucker Prager approximation)

260

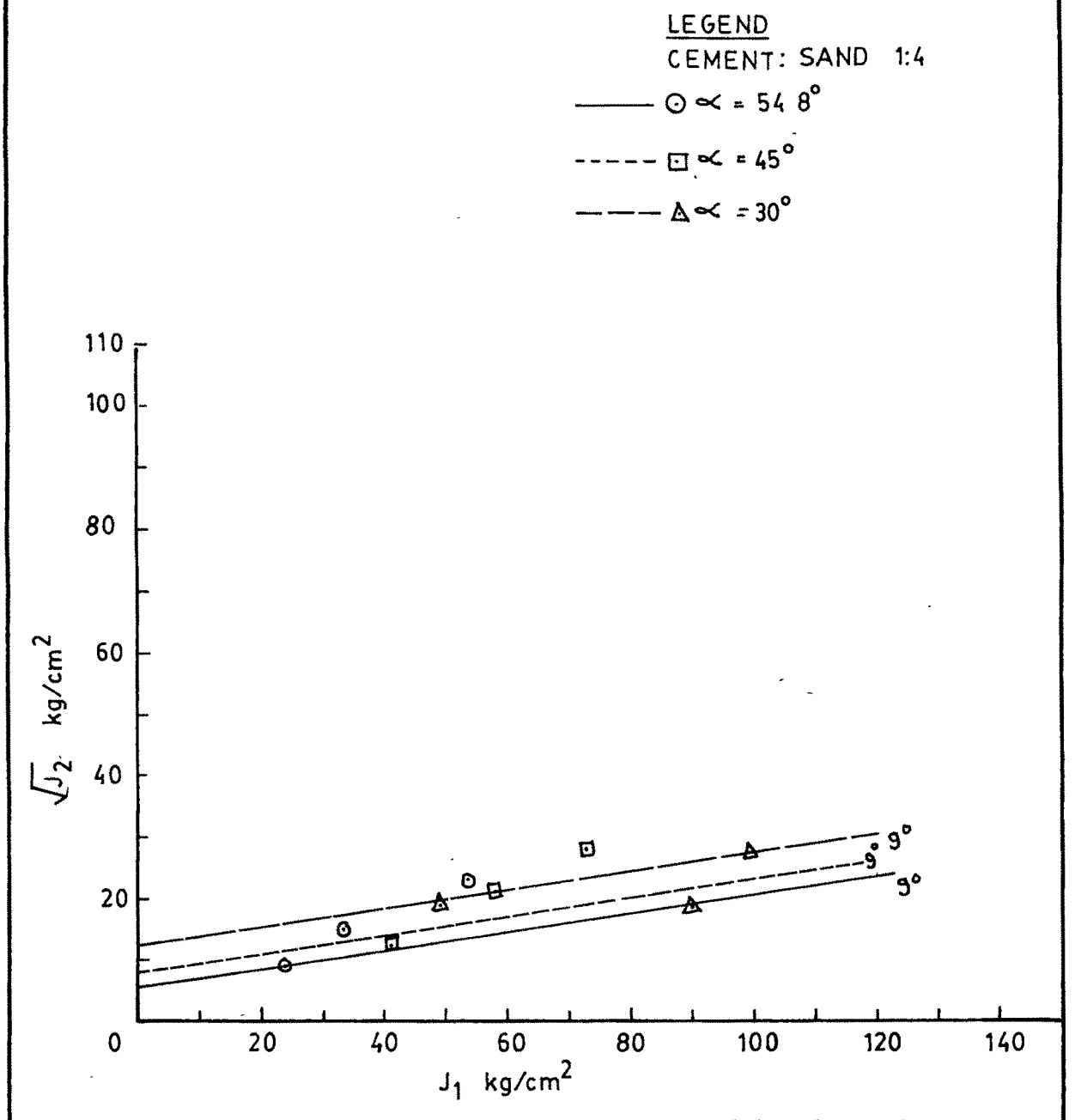

FIG.7·8 A FAILURE ENEVELOPE IN TERMS OF STRESS INVARIENTS
(Drucker Prager approximation)

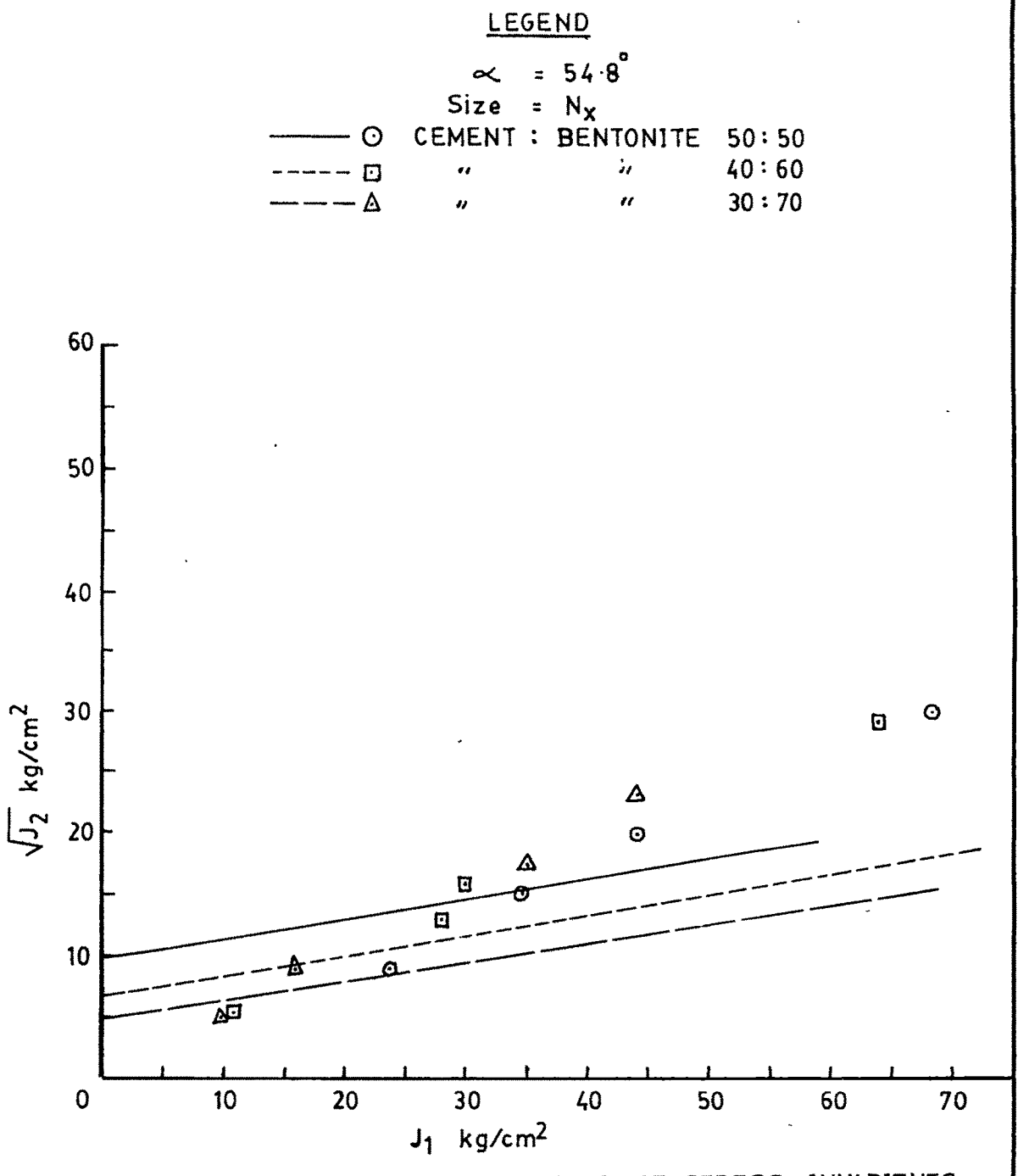

FIG.7·9 A FAILURE ENEVELOPE IN TERMS OF STRESS INVARIENTS
(Drucker-Prager approximation)

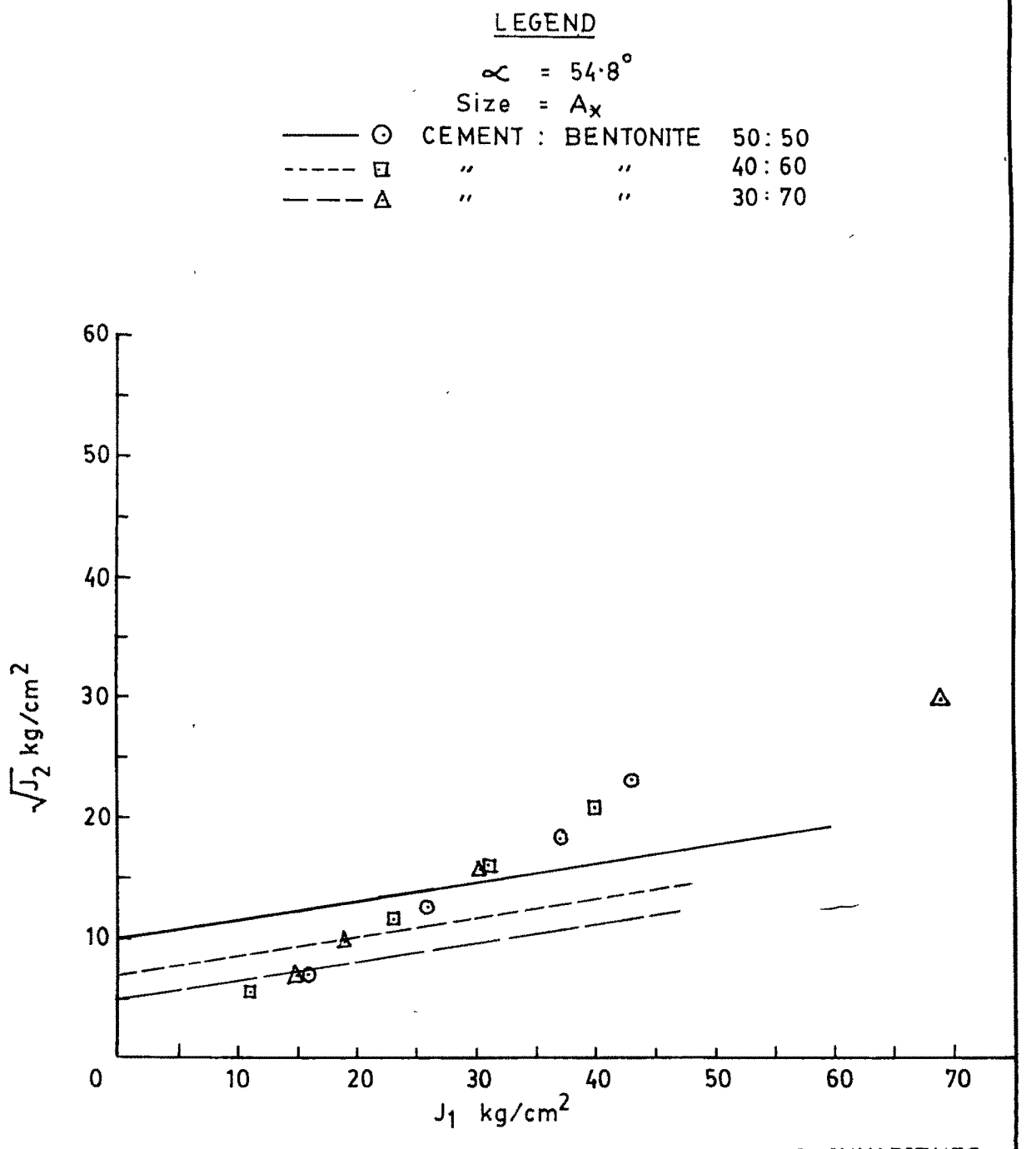

FIG.7-10 A FAILURE ENEVELOPE IN TERMS OF STRESS INVARIENTS
(Drucker-Prager approximation)

fully the mathematical amenability of theory of plasticity a further step in terms of a valid flow rule needs to be discovered from the delineation of pre and post peak phenomena of failure of jointed rocks.

7.3.0. STRESS DEFORMATION CHARACTERISTICS OF JOINTED ROCKS

The most noteworthy feature as was seen from Figures 6.7 to 6.50 is the occurance of the downdard concave behaviour in the early stages of loading indicating the development of non uniform normal stresses. Since the behaviour is noticed in the conventional strain controlled open loading system as well as servo controlled closed loop MTS setup it needs to be investigated as fundamental characteristics of the shearing behaviour in jointed rocks.

A series of loading and unloading cycles at various stress levels upto the peak under triangular and sinusoidal loading revealed (Figures6.49 & 6.50) that the portion of energy is stored elastically while the balance is dissipated plastically throughout the deformation upto the peak stress. The translation of loops bodily with the second cycle of loading at the same stress level signifies that the magnitude of energy dissipation at a particular stress level is fixed with respect to the stress combinations at that point. It can be hypothesised that the stored elastic energy acts as a triggering energy for plastic deformation at every subsequent loading. It will be possible to visulize that as the stress level increases the number of potential sliding contacts increase and the sliding takes place as a result of release of stored energy with an orientation deviating from critical

direction associated with energy spent only in basic friction. Just near the peak stress all the contacts are forced to slide at physically existing plane of sliding, because of bursting out of stored energy a catastrophic failure results. The postulated mechanism of deformation is corroborated from the volumetric strain characteristics where in early parts of loading there is almost negligible volume change while a slight gradual volume change upto the peak and there after occurs a phenomenal volume change (Fig. 6.44 to 6.50). From the solitary (Fig. 6.44 to 6.50) observations on MTS in the post peak region it appears that after the failure of the joint a sliding takes place between the two blocks in a classical manner.

7.4.0. PHENOMENOLOGICAL PARAMETER OF DILATANCY

It was postulated that an additional energy is spent due to sliding at an orientation deviating from the critical orientation solely associated with energy spent in the basic friction. While considering the static equilibrium of two sliding bodies a parameter in terms of a ratio of angle of physical sliding to angle of critical sliding, which is equivalent to the ratio of increment of strains. i.e. instantaneous value of poisson's ratio. Macroscopically the dilatancy parameter is expressed as $\tan\alpha/\tan(45+\phi/2)$ while microscopically it is $(1-\frac{d(\frac{\Delta V}{V})}{d\epsilon_1})$. In conventional setup it is not possible to measure the dilatancy and therefore the former parameter is required to be used. Because of availibility of the MTS setup and possibility of measuring the volume change an attempt was made to observe the dilatancy rate during the deformation of jointed rock specimens. Figure 7.11 and 7.12

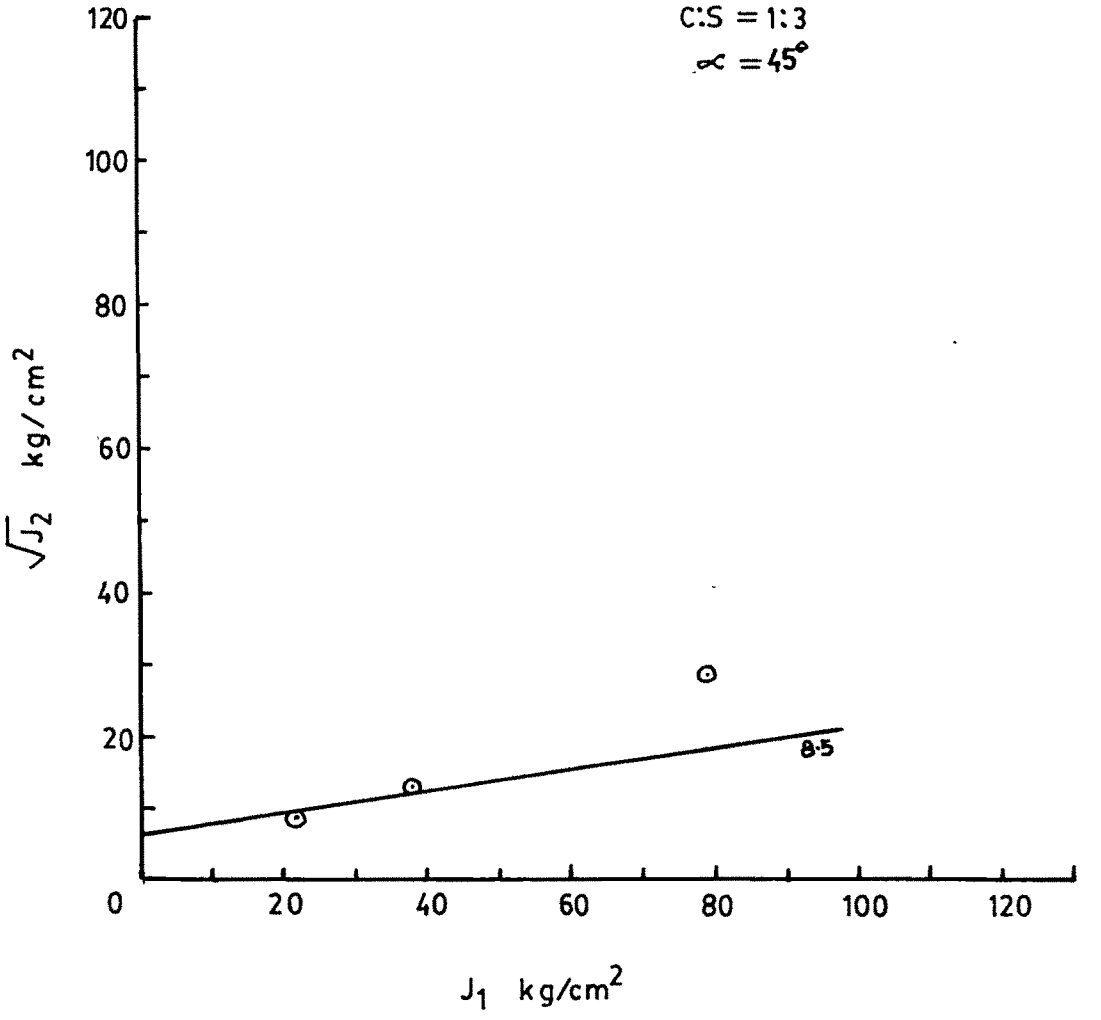

FIG.7·11 A FAILURE ENEVELOPE IN TERMS OF INVARIENTY (Drucker-Prager approximation) TESTED IN M T S SETUP.

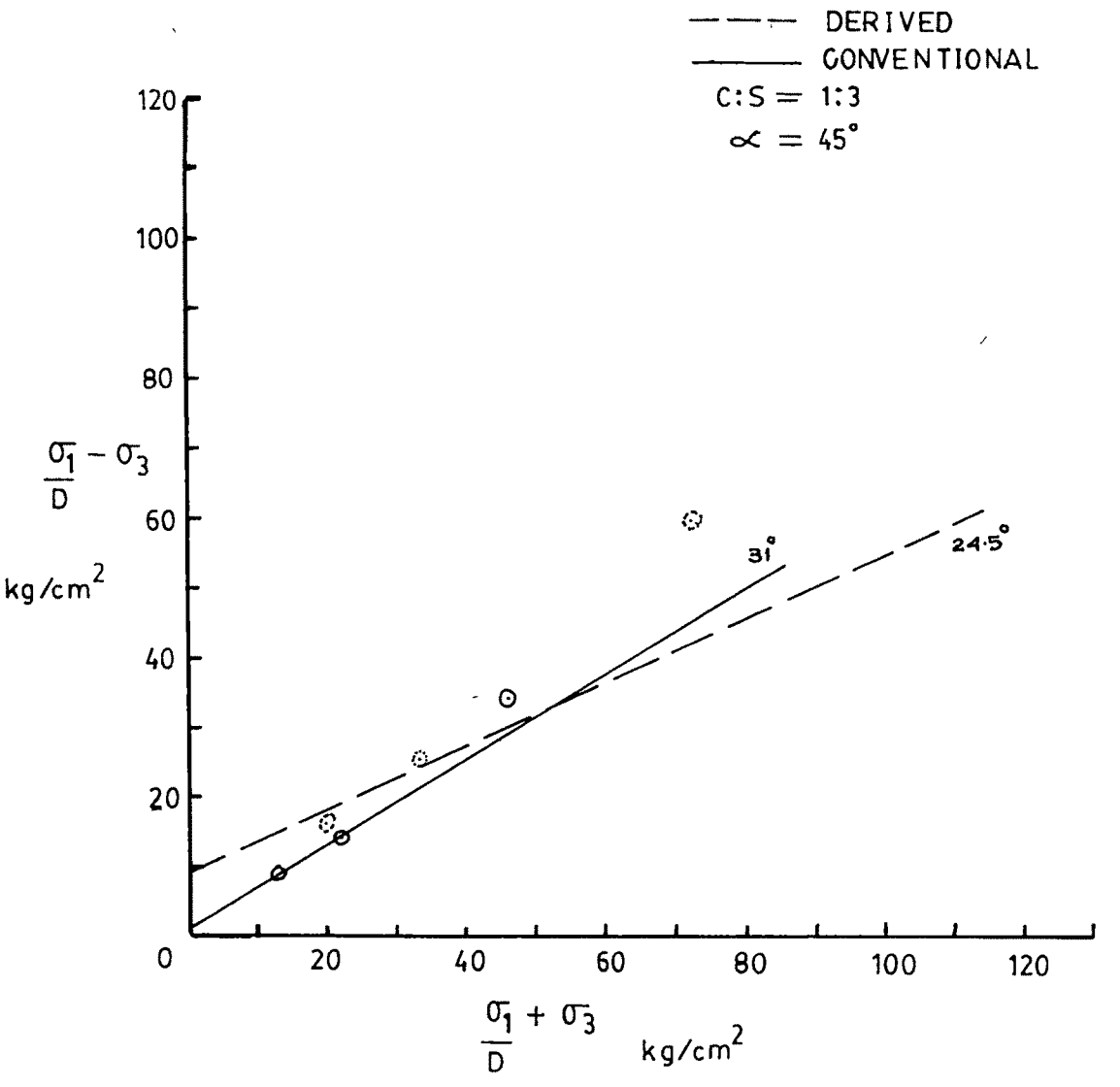

FIG. 7-12 A COMPARISION OF FAILURE ENVELOPES
(TESTED IN MTS SET UP)

represents the comparison of the failure enevlopes worked out using $\tan\alpha/\tan(45+\phi_\mu/2)$ and the $(1-\frac{d(\frac{\Delta V}{V})}{d\epsilon_1})$ from which it is evident that the dilatancy parameter has fundamental basis. Table 7.4 gives the comparison of values of dilatancy parameters. From the table it is evident that the dilatancy parameter worked out from actual observation is in agreement with the calculated dilatancy parameter, in other words, the value of basic friction between the two surfaces taken approximately for the purposes of calculation and analysing the experimental observations is appropriate. The theoretical standing of the dilatancy parameter is established against the experimental investigations. Thus the dilatancy parameter derived during this present investigation turns out to be a phenominological parameter capable to be used in generating the solutions from energy considerations.

7.5.0. INFLUENCE OF JOINT ORIENTATION

The influence of joint orientation on shear parameters ($\overset{*}{C}$, ϕ_μ) determined from the derived failure criterion on the basis of dilatancy and (C_j,ϕ_j) calculated from the failure criterion expressed in terms of stress invariants as per approximation of Drucker-Prager to the Mohr-Coulomb criterion is shown in figures 7.13 and 7.14. It bears out clearly that the angle of basic friction is independent of joint orientation. The cohesion parameters ($\overset{*}{C}$, $\overset{*}{C}_j$) follow parabolic curve with respect to joint orientation which corroborate the stipulation of transference of dilatancy effect on the cohesion value. Further the plots for shear stress at failure against joint orientation as presented in figures

TABLE - 7.4

Sr. No.	Designation	Dilatancy $\frac{\tan \alpha}{\tan(45+\phi_\mu/2)} (1-\frac{d(\frac{\Delta v}{v})}{d\epsilon_1})$		ϕ_μ Assumed	ϕ_μ Actual
1	2	3	4	5	6
1	$B_4^{54.8*}$	0.852	0.848		
2	$B_4^{54.8**}$	0.852	0.896	28°	27°
3	$B_4^{54.8***}$	0.852	0.865		
4	B_2^{45*}	0.601	0.606		
5	B_4^{45*}	0.601	0.630	28°	27°
6	B_6^{45*}	0.601	0.604		
7	B_4^{30*}	0.961	0.978	28°	28°

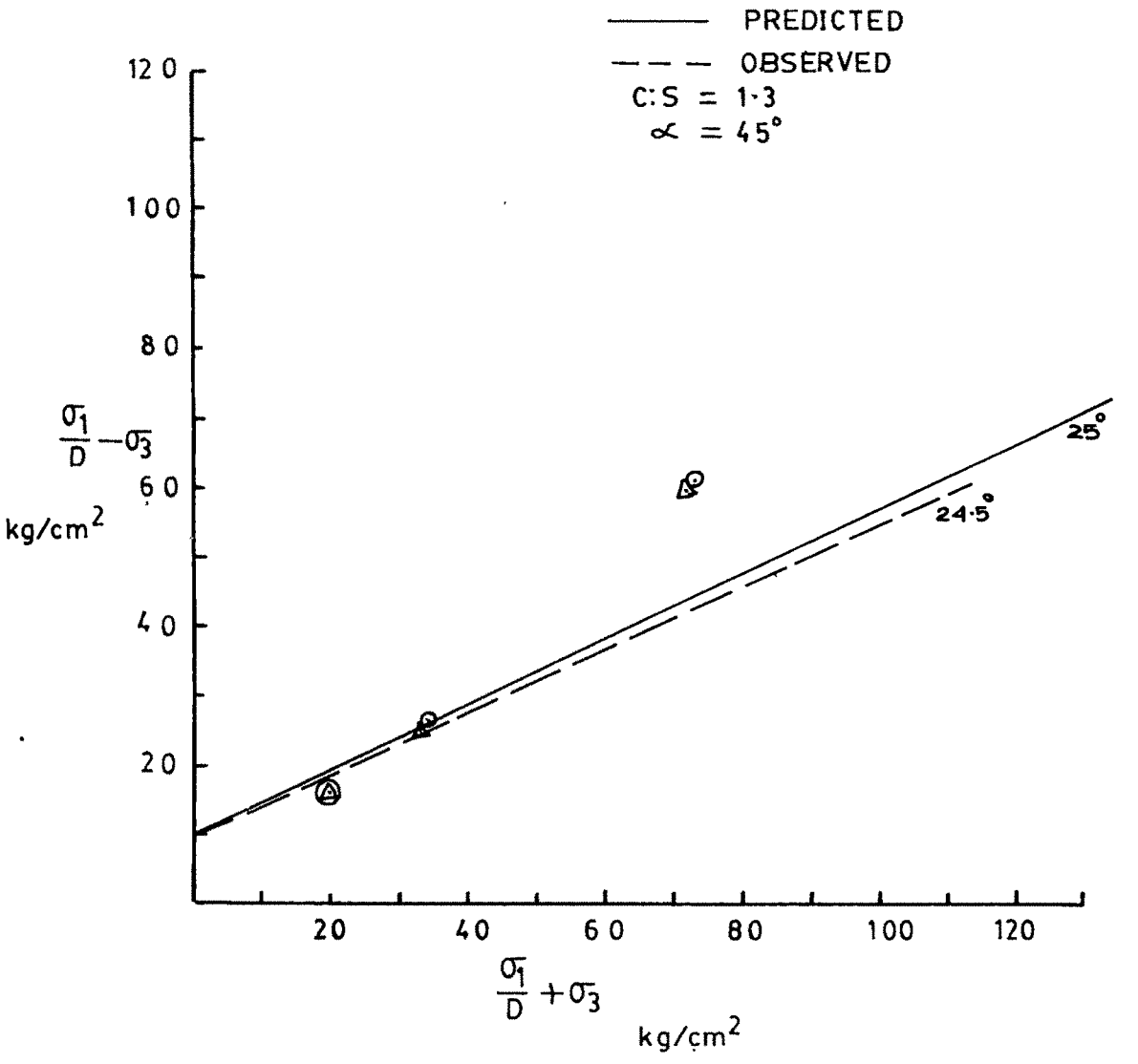

FIG. 7·13 FAILURE ENVELOPES WITH DILATANCE PREDICTED VALUE AND OBSERVED VALUE IN MTS SET-UP

270

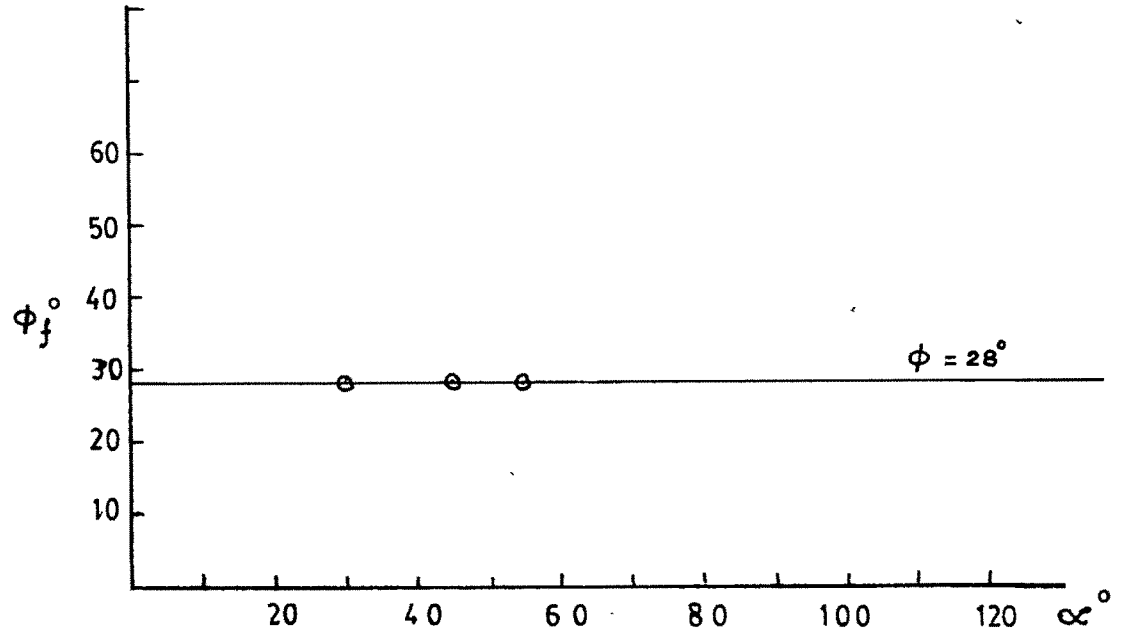

FIG. 7·14(a) INFLUENCE OF JOINT ORIENTATION ON SHEAR PARAMETERS OF DERIVED FAILURE CRITERION

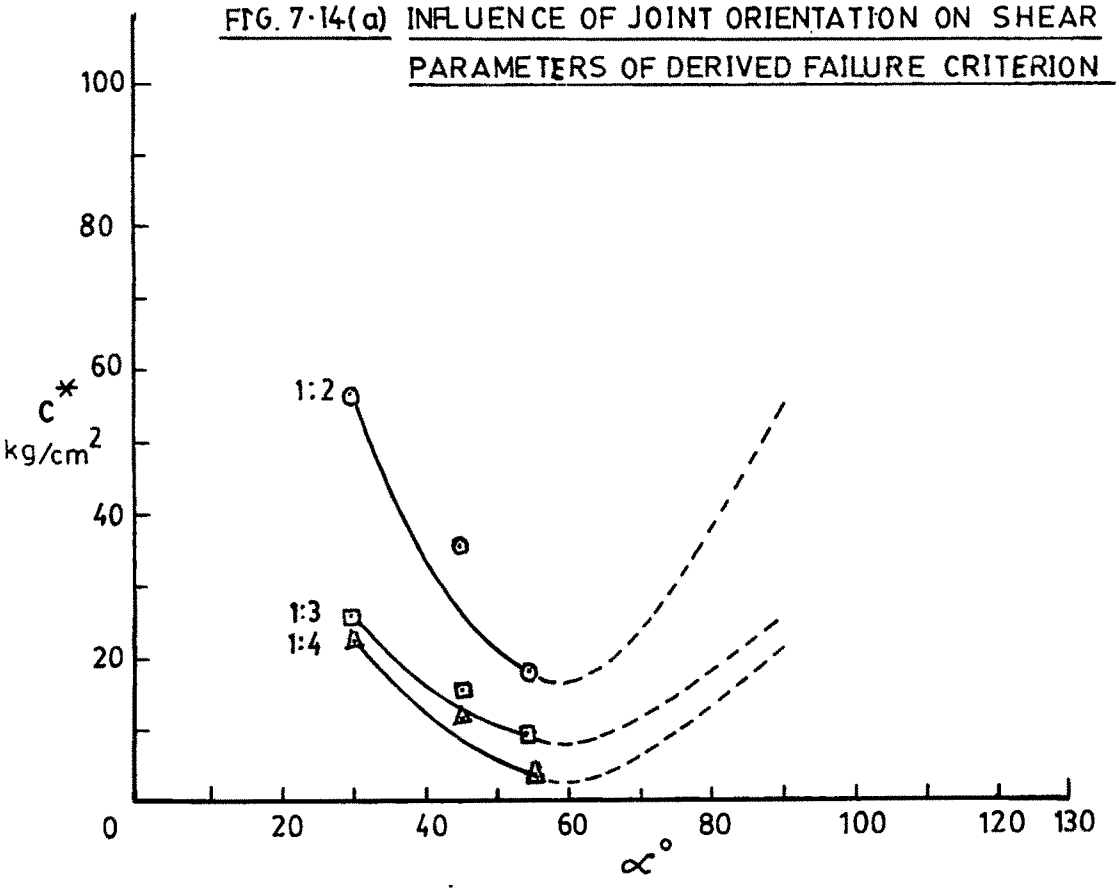

FIG. 7·14(b) INFLUENCE OF DERIVED OF JOINT ORIENTATION ON SHEAR PARAMETERS OF DERIVED FAILURE CRITERION

7.15 to 7.17 for cement:sand gouge material reveal parabolic nature with respect to joint orientation with a minimum occuring around 60° from extrapolation which conforms to the trend predicated as per the proposed theoretical model. It is clearly evident that if the dilatancy effect is excluded the angle of friction is analogous to the angle of basic friction irrespective of joint orientation. The effect of inclination therefore is only on the cohesion parameters of the shear strength coroborating the concept of transference of dilatancy effect on the cohesion parameters. Coulomb's criterion corrosponds to dilatancy parameter equal to unity which can occur whence the critical direction $(45 + \phi_\mu/2)$ coincides with the joint orientation. Thus the Coulomb criterion is a particular case of the derived failure criterion for a condition of no volume change.

7.6.0. INFLUENCE OF GOUGE MATERIAL

Plots 7.19, 7.20 show the cohesion values as per Mohr-Coulomb with dilatancy modified stresses ($\overset{*}{C}$) and on the basis of Drucker-Prager approximation with dilatancy modified stress (C_j). According to these plots the cohesion values are function of compressive strength of gouge material, the effect becomes more pronounced as the strength of the fill material increases. It can be noted the C_j values do not evince appreciable change in comparison to $\overset{*}{C}$ values. For softer materials Drucker-Prager approximation circumscribing the Mohr-Coulomb criterion holds while for harder material inscribing condition prevails. In terms of adopting Drucker-Prager approximation for analysing on the basis of limit

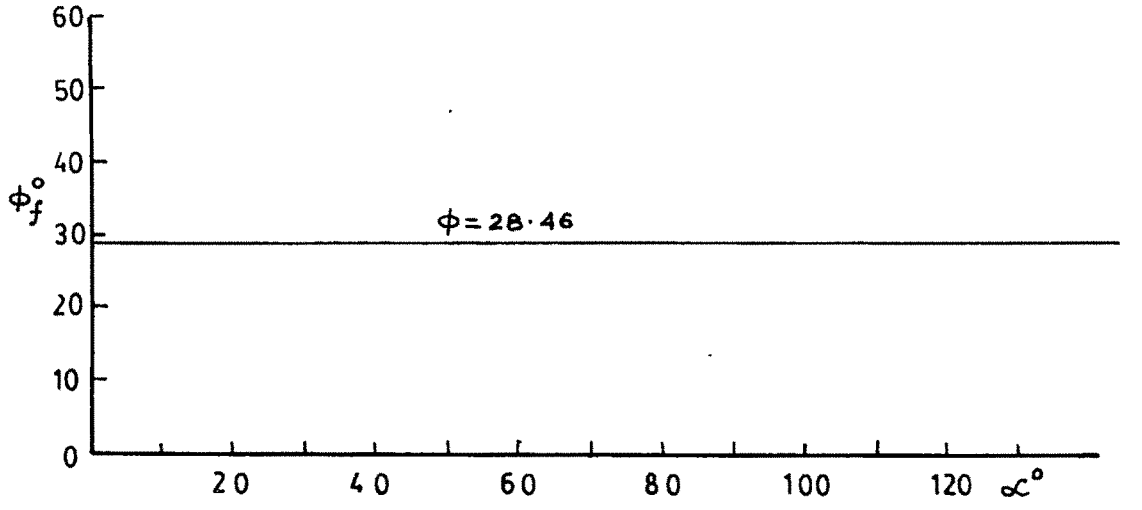

FIG.7·15(a) INFLUENCE OFJOINT ORIENTATION ON SHEAR PARAMETERS OF FAILURE CRITERIAN IN STRESS INVARIENTS

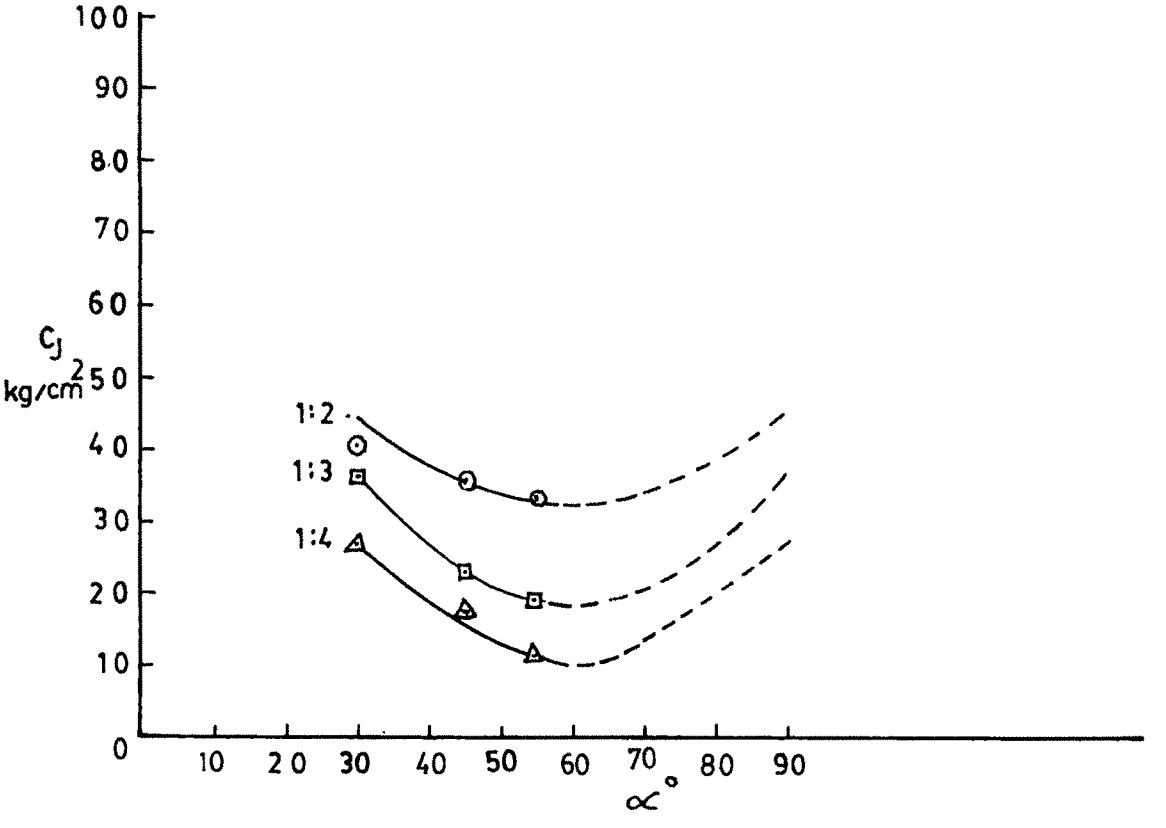

FIG.7·15(b) INFLUENCE OF JOINT ORIENTATION ON SHEAR PARAMETERS OF FAILURE CRITERIAN INSTRESS INVARIENTS

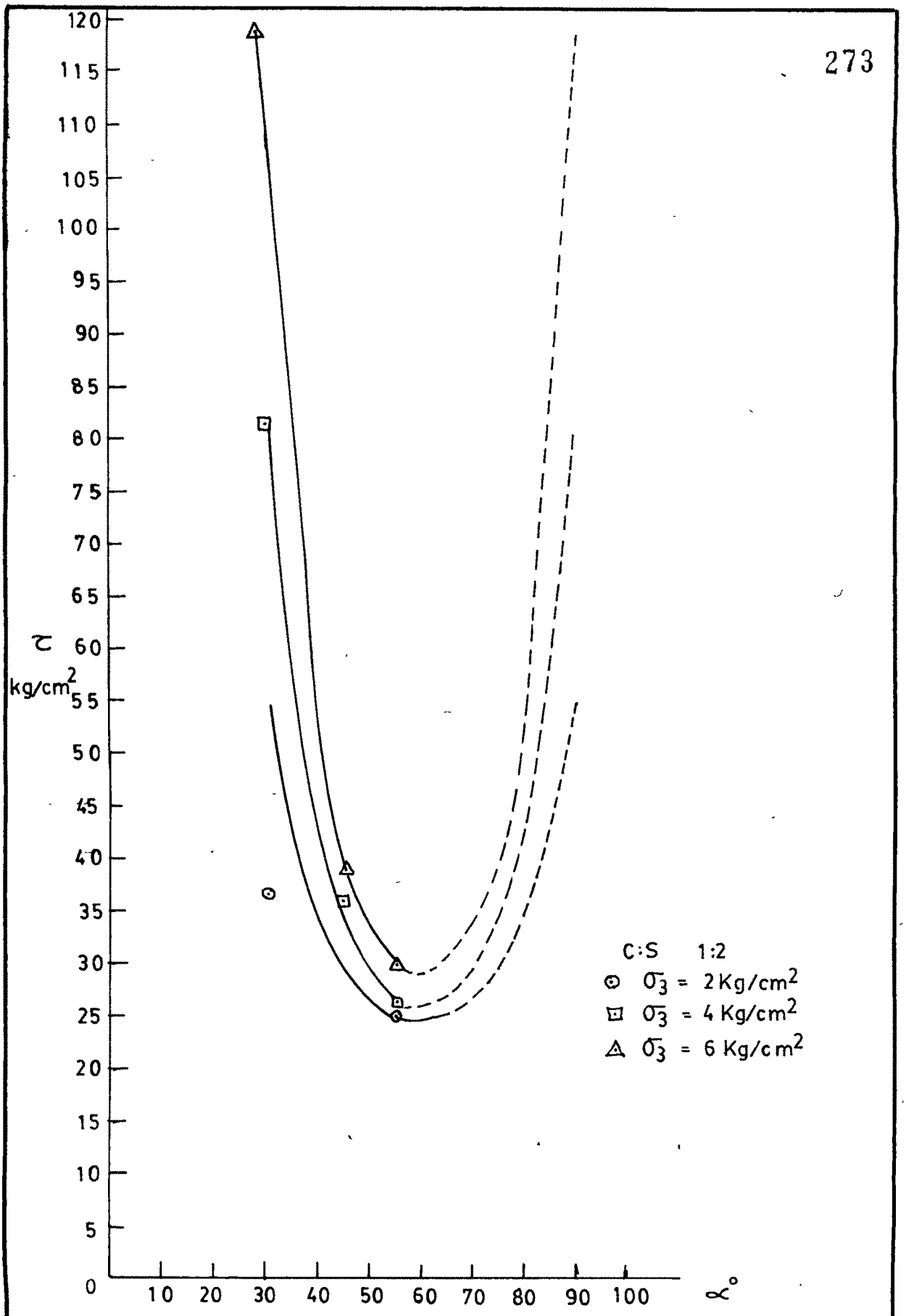

FIG.7.16 RELATIONSHIP BETWEEN SHEAR STRESS AT FAILURE & JOINT ORIENTATION

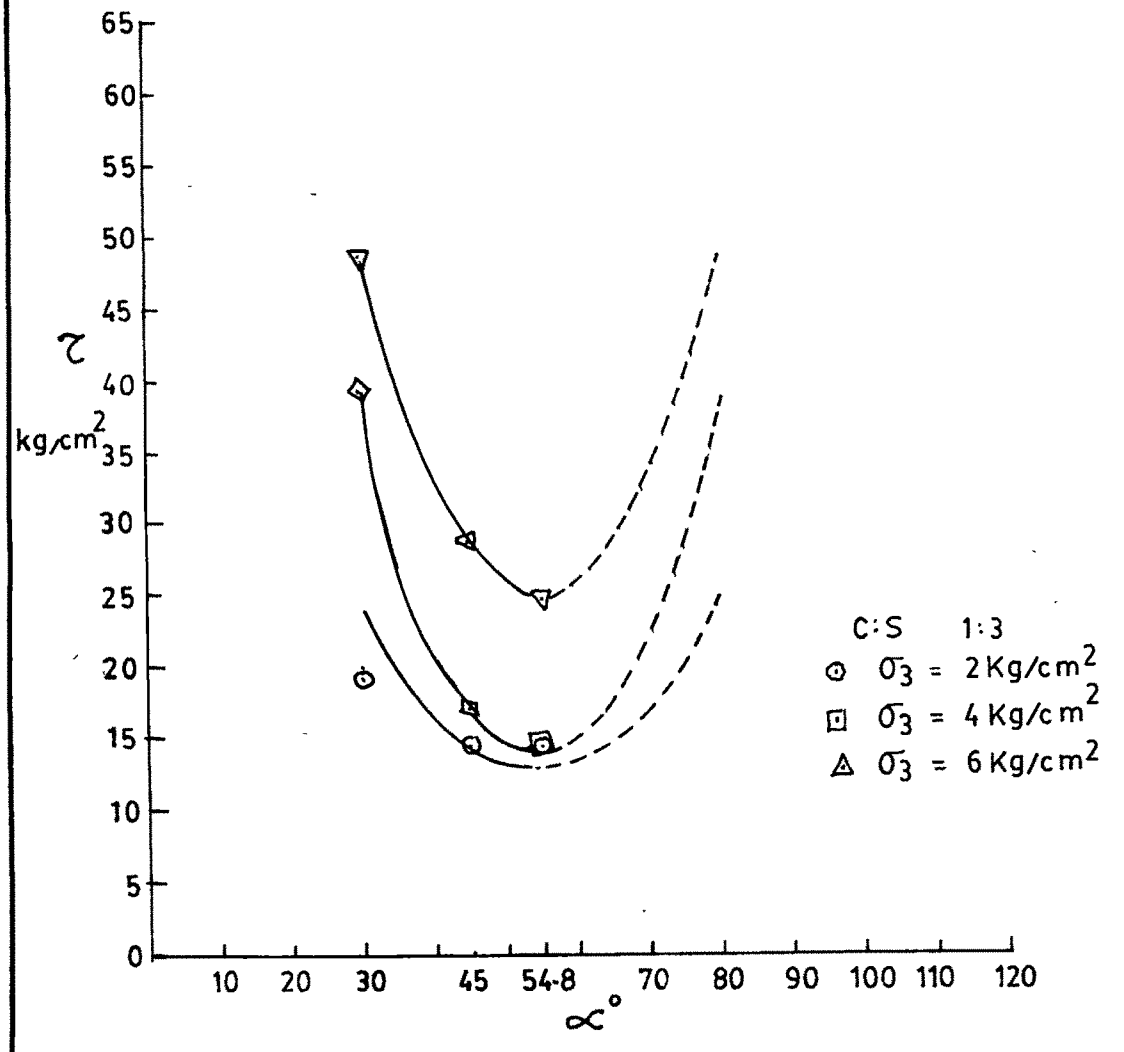

FIG.7-17 RELATIONSHIP BETWEEN SHEAR STRESS AT FAILURE AND JOINT ORIENTATION

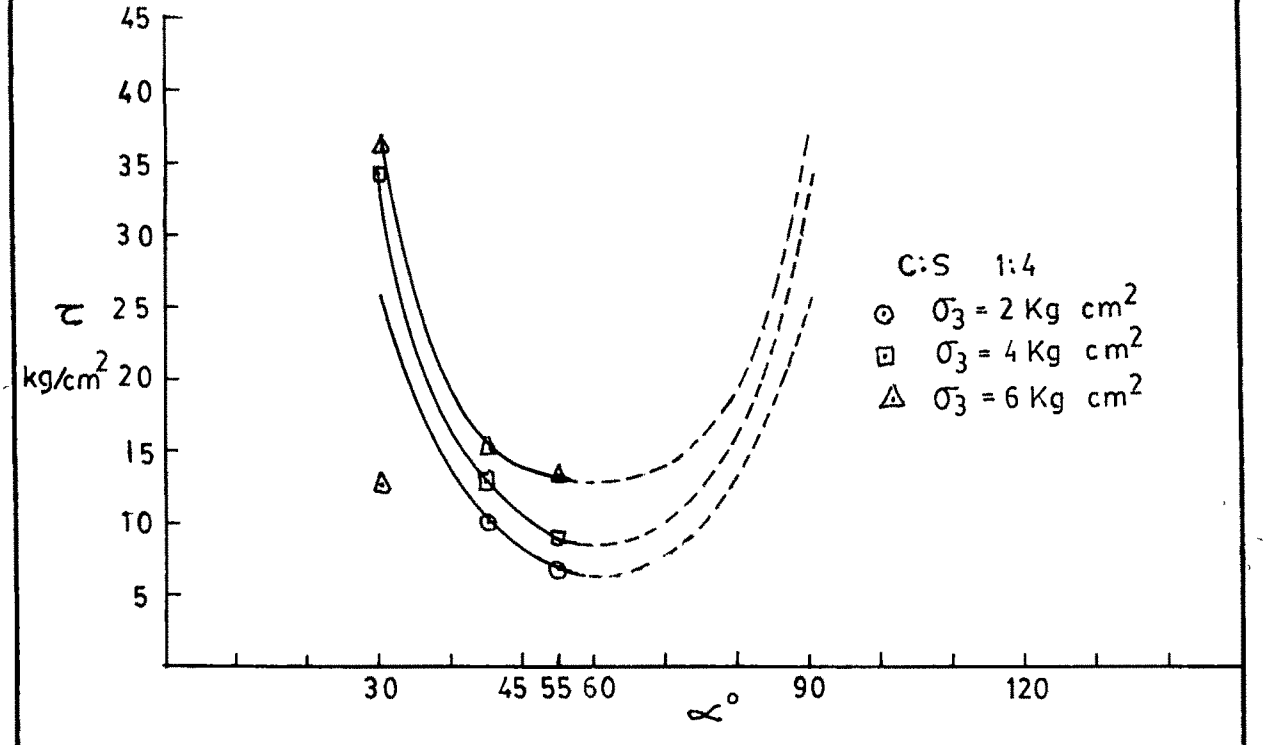

FIG. 7.18 RELATIONSHIP BETWEEN SHEAR STRESS AT FAILURE AND JOINT ORIENTATION

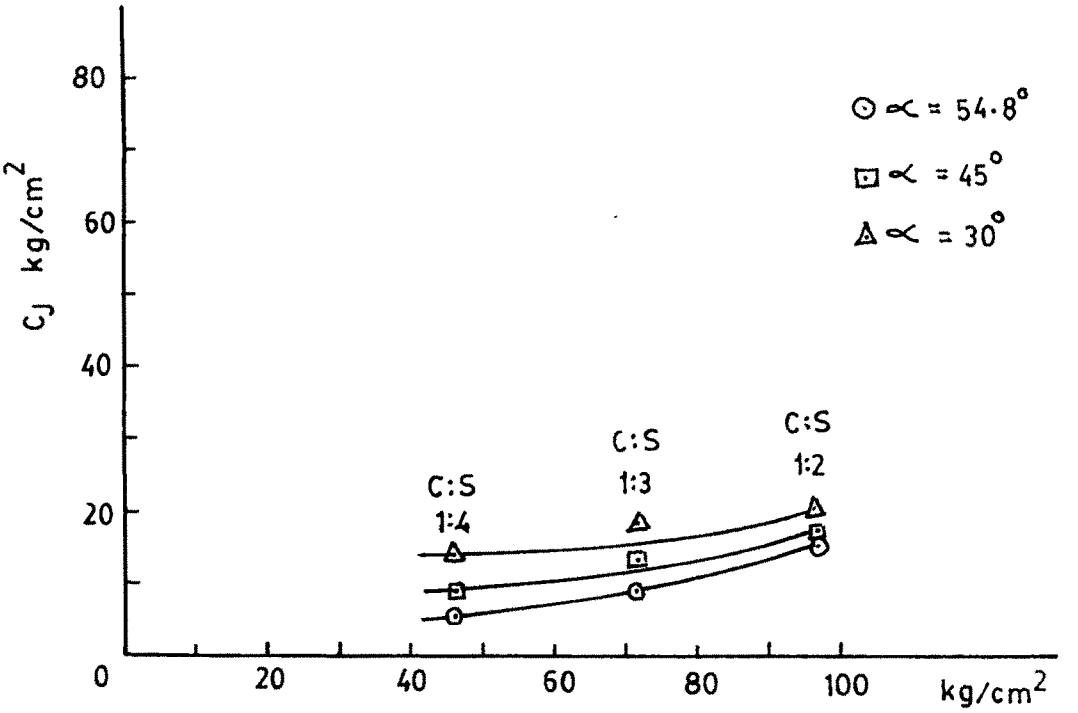

FIG.7·19(a) INFLUENCE OF STRENGTH OF GOUGE MATERIAL ON COHESION PARAMETER.

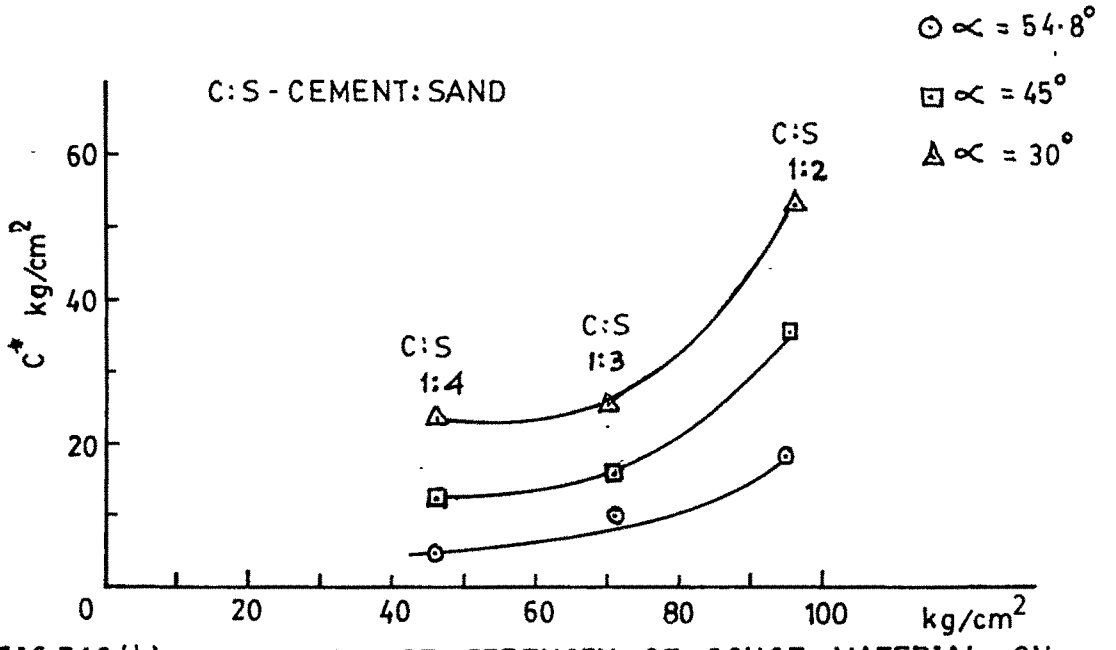

FIG.7·19(b) INFLUENCE OF STRENGTH OF GOUGE MATERIAL ON COHESION PARAMETER

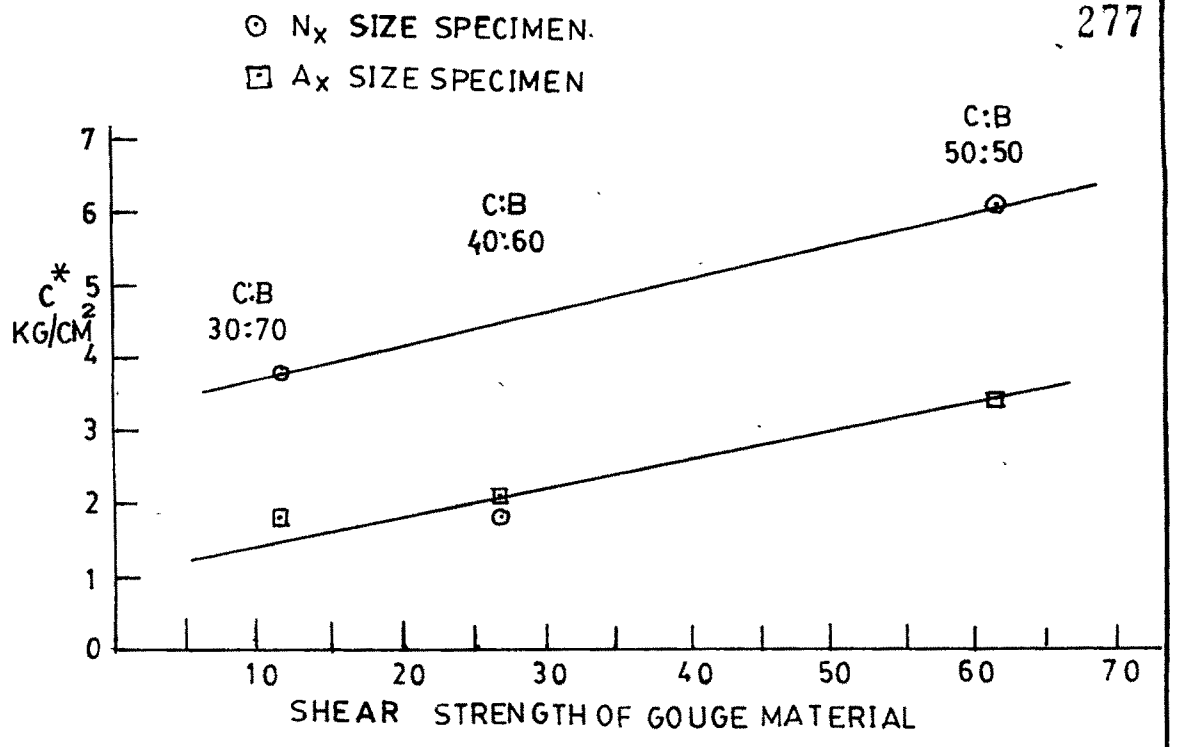

FIG.7·20(a) INFLUENCE OF STRENGTH OF GOUGE MATERIAL ON C^* PARAMETER

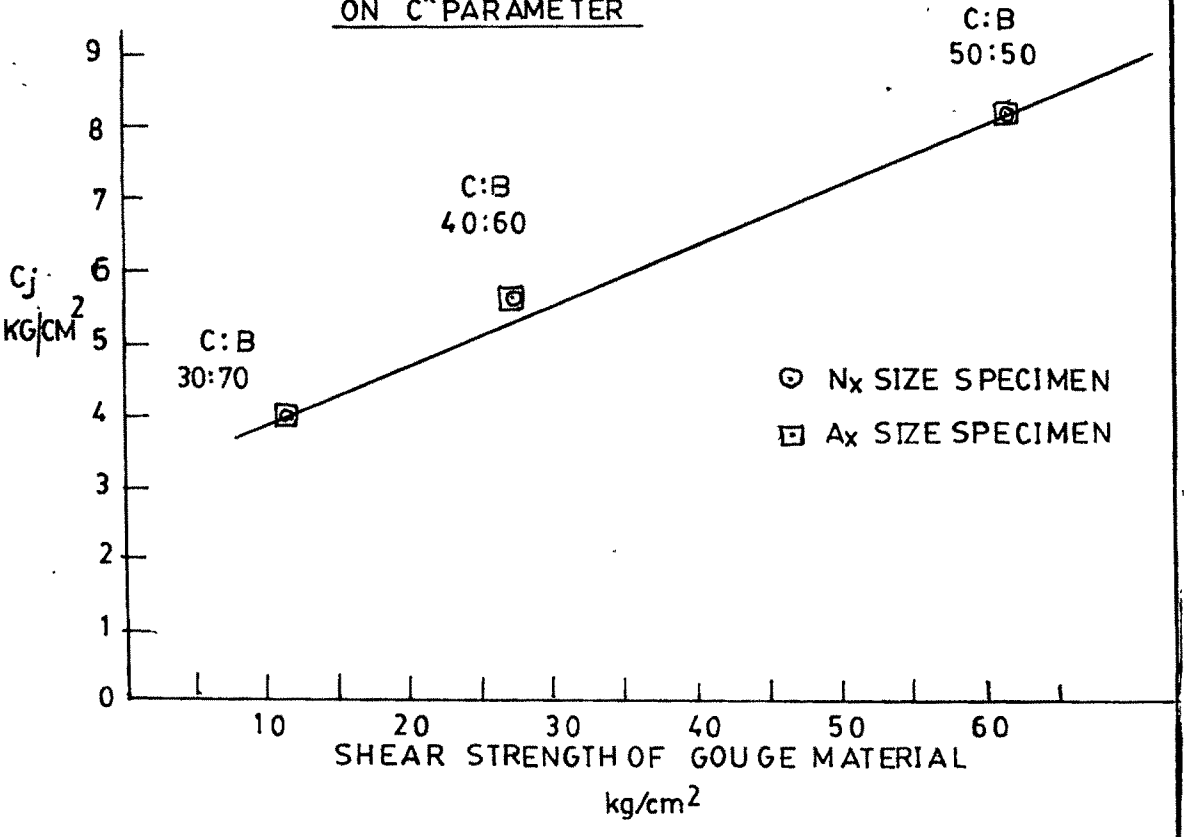

FIG. 7·20(b) INFLUENCE OF STRENGTH OF GOUGE MATERIAL ON C_j PARAMETER

equilibrium conservative values of factor of safety will be computed in case of harder materials while it will be just contrary in case of softer materials.

7.7.0. INFLUENCE OF SCALE

Figures 7.21 to 7.23 show a relationship between a octohedral shear and octohedral normal stress obtained from the experimental observations from tests conducted on N_x and A_x size specimens with joint orientation 54.8° corresponding to approximately unit dilatancy for gouge material cement:Bentonite with ϕ_μ = 21° having proportions 50:50,40:60 and 30:70 to determine the effect of scale on the critical combinationof of stresses at the point of failure. For a scale ratio of about two which corrosponds to about three times in terms of contact area, the influence is perceptible even if the allowance is permitted for the reasonable variations in the measurements. The stress-strain characteristics portrayed in fig6.24 to 6.31 also show clearly the influence of the size throughout the deformation of the specimens. On the failure envelope the influence is on the cohesion parameter for N_x and A_x size with gouge material proportions 50:50, 40:60 and 30:70 respectively. In view of the exposition it would be pertinent to investigate the influence of scale on the stress deformation behaviour of jointed rocks.

7.8.0. CONCLUSIONS

The most significant and pertinent conclusions from the point of view of establishment of a theoretical model which can be exploited for developing a failure criterion and

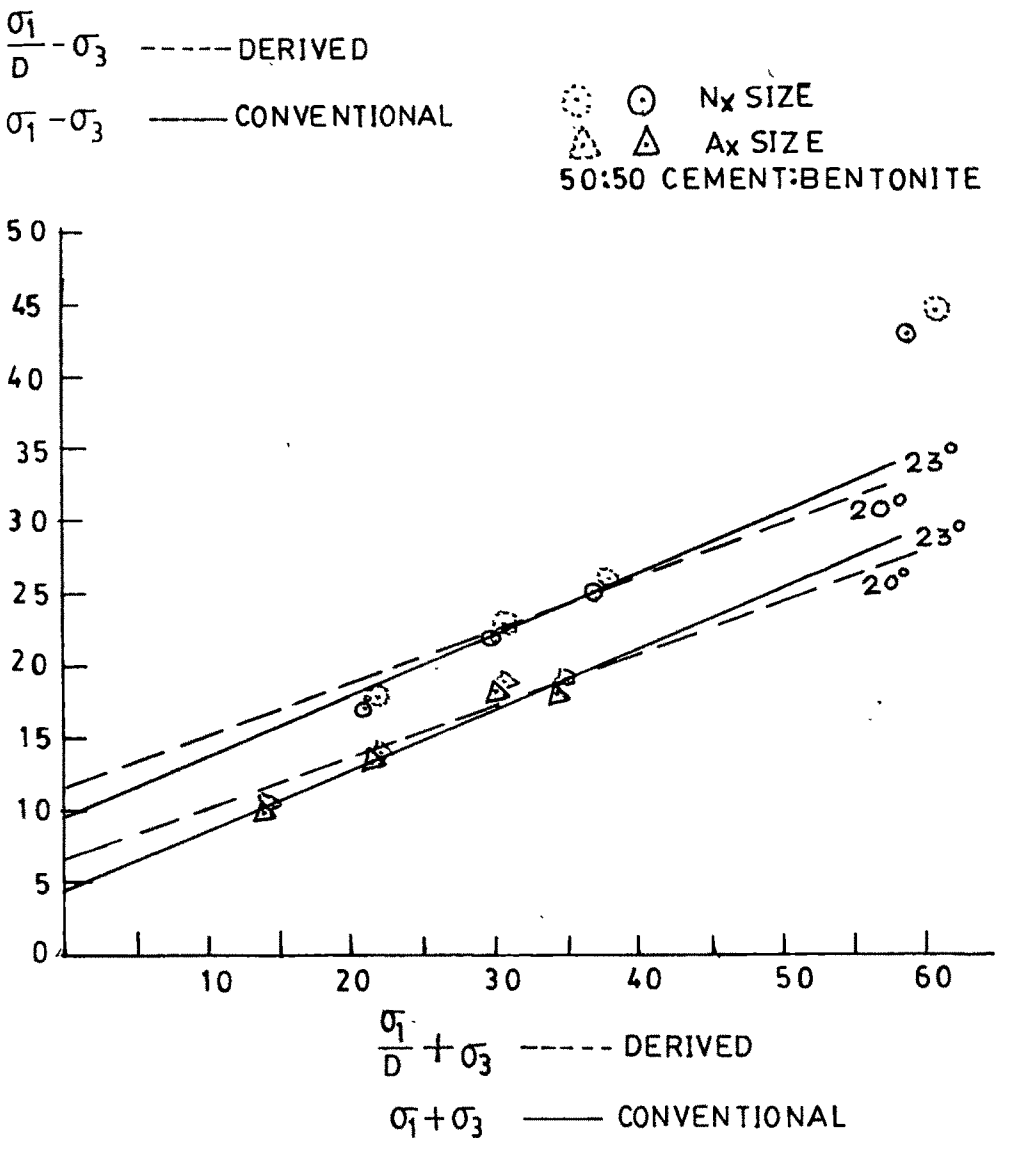

FIG. 7·21 COMPARISION OF FAILURE ENVELOPES FOR Nx AND Ax SPECIMENS

280

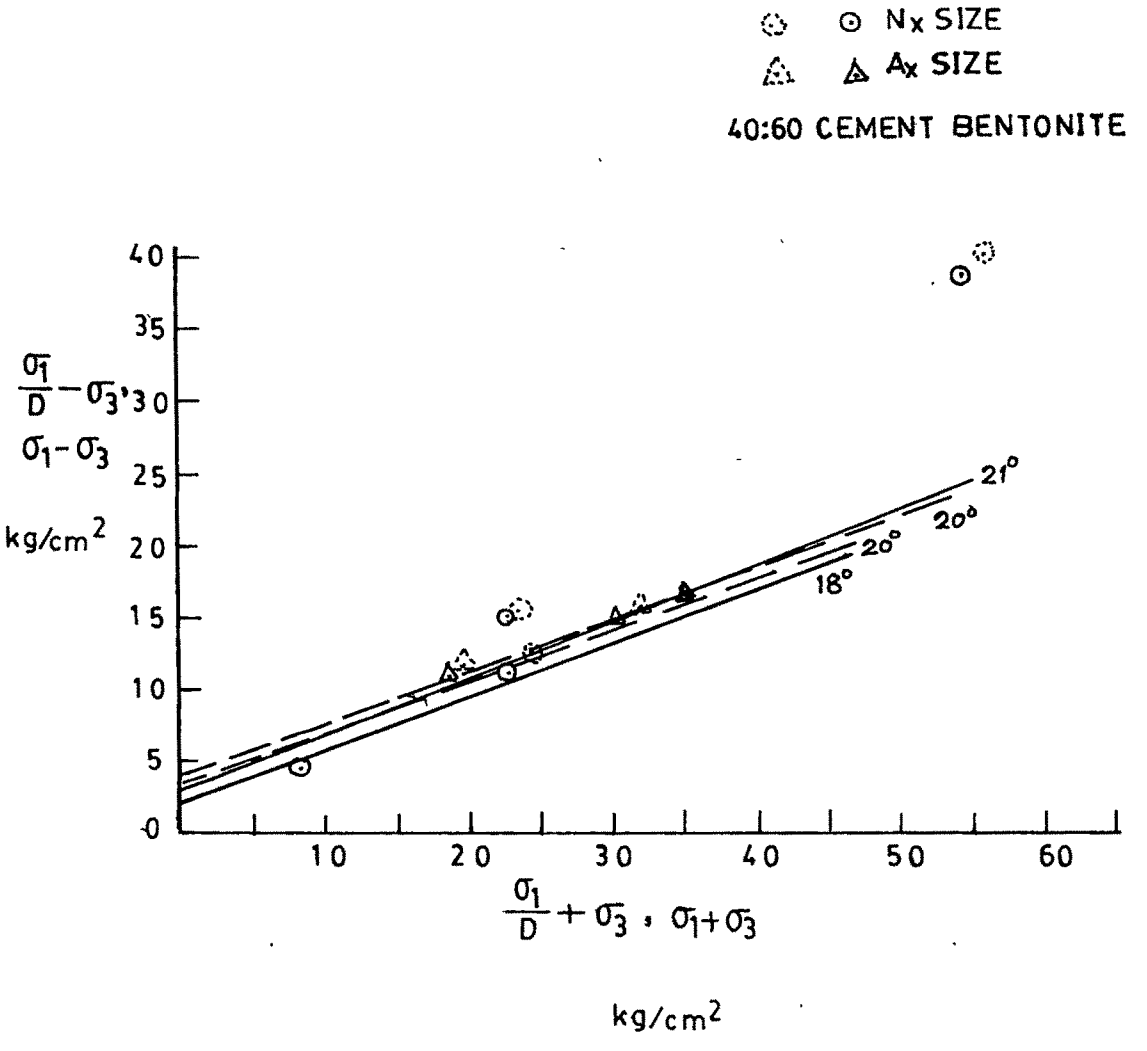

FIG.7·22 COMPARISION OF FAILURE ENVELOPES FOR N_X AND A_X SIZE SPECIMENS

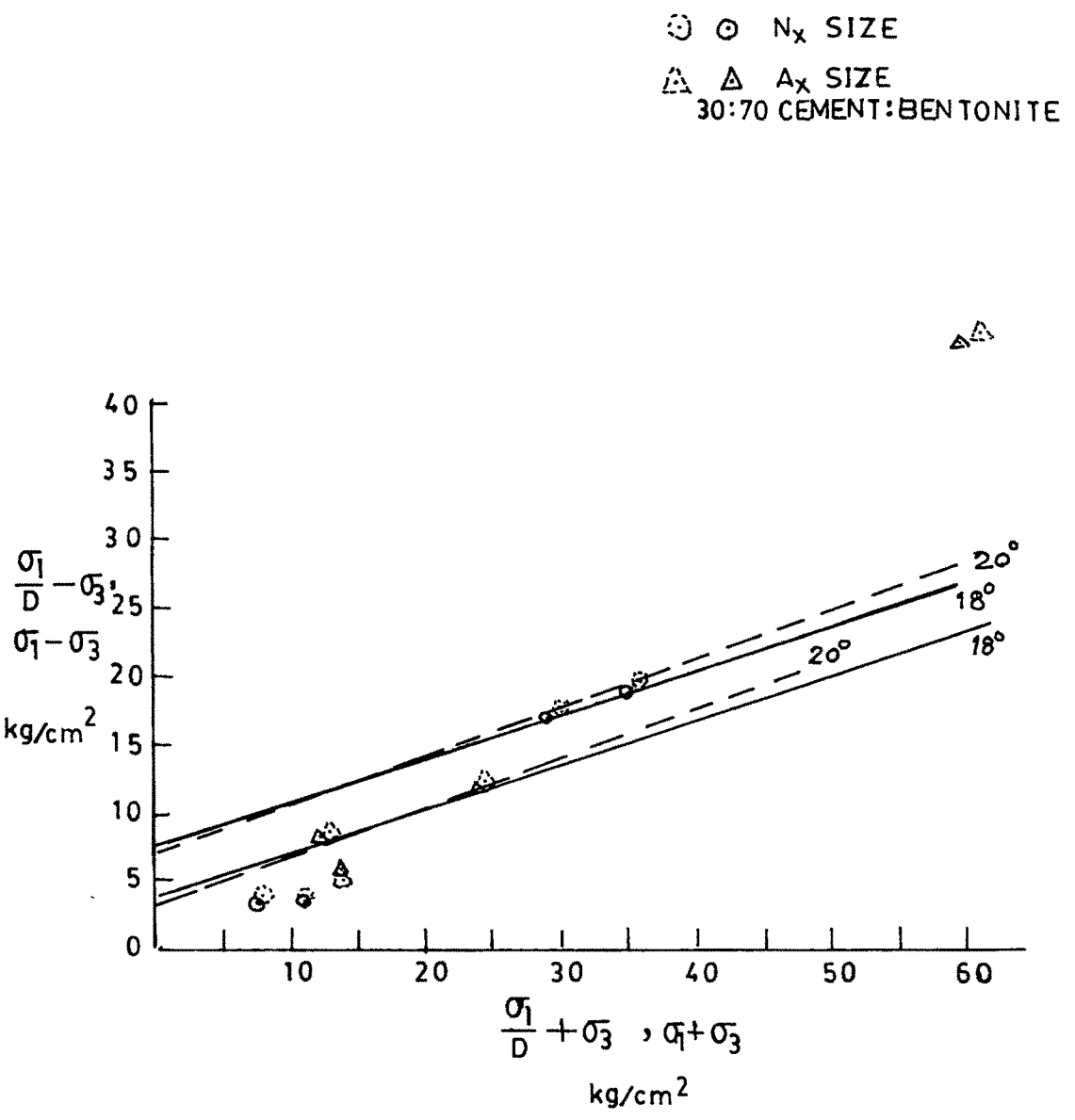

FIG.7-23 COMPARISION OF FAILURE ENVELOPES FOR N_X AND A_X SIZE SPECIMENS

associated constitutive properties for understanding the mechanical behaviour of jointed rocks and their prospective use in the solution schemes for varieties of boundary value problems in engineering practice are presented as below:

* The physical model of a body sliding on an inclined plane when analysed for static equilibrium yield a criterion for failure in a jointed rock, on the hypothesis that the minimum energy in friction is dissipated only in sliding at a critical angle $45 + \phi_\mu/2$ with major principal plane and the exccess energy due to deformation associated with volume change is in sliding at an orientation deviating from the critical orientation. The failure stress is expressed into two independent parameters, one associated with basic friction and another associated with geometry. When expressed interms of stress invariants and on applying the approximation of Drucker-Prager lead to a convenient expression for a criterion of failure for jointed rock mass. The identification of the behaviour of jointed rock into the theoretical framework of plasticity furnish a sound base for further theoretical developments. The failure criterion so derived stand verified for the principal factors governing the shearing behaviour of jointed rocks.

* The dilatancy is the principal phenomenon during the shearing of a jointed rock the quantum of which at the point of failure is the ratio between tangents of joint orientation and the critical orientation. From geometrical consideration this ratio is equivivalent to the ratio of lateral strain to axial strain at the point of failure.

The validity of the dilatancy parameter is also established from the experimental observations of volume change during the shearing of jointed rocks.

* The mechanistic picture for shearing behaviour in jointed rock mass is that initially the energy is stored elastically due to compression of contacts and whence the ratio of tangential stresses to the normal stresses approach a critical friction value the plastic sliding takes place whose direction gets modified owing to the stored elastic energy and ultimately forced to slide on an orientation deviating from the critical orientation. The loading and unloading behaviour as observed in specially conducted experiments corroborate the conceptulized mechanism.

* Joint orientation and gouge material characteristics are the significant factors which governs the shearing behaviour of jointed rocks since the principal phenomena of dilatancy is a function of these two factors. The conventional method of stability analysis based on classical Mohr-Coulomb criterion which ignores the volume change needs to be modified by incorporating the dilatancy parameter.

* In view of possibility of applicability of theory of plasticity owing to validity of Drucker-Prager approximation to the Mohr-Coulomb failure criterion modified for dilation and the probable mechanistic model for deformation comprised of elastic and plastic components it should be possible to develop a constitutive relationship for its use in the solution techniques for analysing the various boundary value problems in the area of jointed rocks.